ELSEVIER

Chemical Geology 172 (2001) 307–329

CHEMICAL GEOLOGY
INCLUDING
ISOTOPE GEOSCIENCE

www.elsevier.com/locate/chemgeo

Isotopic disequilibrium in marine calcareous algae

Dongho Lee [a,*], Scott J. Carpenter [b]

[a] *Ottawa-Carleton Geoscience Center, University of Ottawa, Ottawa, ON, K1N 6N5 Canada*
[b] *Department of Geoscience, Paul H. Nelson Stable Isotope Laboratory, University of Iowa, 121 TH, Iowa City, IA, 52240-1379, USA*

Received 28 April 1998; accepted 17 March 2000

Abstract

A survey of the $\delta^{13}C$ and $\delta^{18}O$ values of $CaCO_3$ precipitated by marine calcareous algae was conducted to examine 'vital effects' produced by the various styles of calcification of the major algal subdivisions (Codiacea, Dasycladacea, Coralline algae and Calcareous red algae). Algae are categorized on the basis of stable isotope ratios and styles of calcification. Styles of calcification and associated processes in these plants are diverse and produce a wide range of $\delta^{13}C$ values that are both lower and higher than predicted equilibrium values (from approximately $-6‰$ to $+8‰$). In general, $\delta^{13}C$ values of algal carbonate reflect phylogenetic and ontogenetic changes in photosynthesis that produce changes in the $\delta^{13}C$ value of the calcifying fluid due to modification of the photosynthesis/respiration ratio. $\delta^{18}O$ values are less variable, and in many cases, approximate predicted equilibrium values.

Kinetic fractionation of carbon and oxygen isotopes associated with hydroxylation of CO_2 is observed in the carbonates of *Neogoniolithon* sp. and *Bossiella* sp., where $\delta^{13}C$ and $\delta^{18}O$ values are positively correlated. This positive correlation is similar to trends observed in many carbonate-secreting organisms. Stable isotope data from green algae (Codiaceans and Dasycladacean) are related to the style of each species calcification (i.e., microenvironment of calcification site). Intercellular calcification in *Halimeda* sp. and *Udotea* sp. is characterized by significant metabolic effects in carbonate $\delta^{13}C$ values (up to 7‰ variation within a specimen). Extracellular calcification in *Acetabularia* sp. and sheath calcification in *Penicillus* sp. have carbonate $\delta^{13}C$ and $\delta^{18}O$ values that are near predicted equilibrium values (similar to inorganic precipitates). The $\delta^{13}C$ values of coralline algae are lower than Codiacean green algae by as much as 14‰. We suggest that this difference is due largely to the unique ontogeny of coralline algae. Calcification in the younger portions of coralline algae occurs under strong influence of respiration. Carbonate from *Amphiroa* sp. and *Galaxaura* sp. has relatively invariant $\delta^{18}O$ values that may be useful proxies of ambient conditions.

Keywords: Calcareous algae; Calcification; Vital effects; $\delta^{13}C$ and $\delta^{18}O$ values

1. Introduction

The $\delta^{13}C$ and $\delta^{18}O$ values of marine carbonates can provide useful information regarding the ambient conditions of formation and deposition. For the $\delta^{13}C$ and $\delta^{18}O$ values of biogenic carbonates to be effective proxies of ambient fluid conditions, it is first necessary to understand the various biological fractionations or 'vital effects' associated with carbonate precipitation (e.g., Urey et al., 1951; Swart, 1983; McConnaughey, 1989a,b; Carpenter and Lohmann,

* Corresponding author. Fax: +1-613-562-5192.
E-mail address: dlee@science.uottawa.ca (D. Lee).

0009-2541/01/$ - see front matter
PII: S0009-2541(00)00258-8

1995). However, the literature describing biological fractionation in calcareous organisms is dominated by studies of marine animals. As a result, relatively little is known about how most marine algae fractionate carbon and oxygen isotopes during calcification (e.g., Wefer and Berger, 1991). As the majority of shallow marine carbonates are produced by calcareous algae and corals (e.g., Milliman, 1993), there is a need to better understand the physiology of calcification in these organisms. Our study attempts to provide an understanding of the major variables that control calcification and stable isotope ratios of carbonates in marine calcareous algae. This, in turn, will improve our understanding of calcification in tropical, shallow marine environments and the carbon isotope ratios used to model the marine carbon system.

Our study surveys the $\delta^{13}C$ and $\delta^{18}O$ values of a variety of modern, marine, calcareous algae to characterize the systematic 'vital effects' in these organisms. Calcareous algae are well suited for such studies as they have simple internal structures and their physiology is relatively well documented (e.g., Dawes, 1981; Johansen, 1981). As a result, biologic processes associated with skeletogenesis can be readily observed. This study has two objectives. (1) Carbon and oxygen isotope data obtained from naturally occurring calcareous algae are used to describe the nature of 'vital effects' in these organisms. For this, we have collected skeletal carbonate $\delta^{13}C$ and $\delta^{18}O$ values from representative species of marine calcareous algae such as Codiacean and Dasycladacean green algae, coralline algae and calcareous red algae. For some important species, $\delta^{13}C$ values of the organic matter were also measured. The isotope data of each specimen are interpreted on the basis of available physiological information and proposed calcification mechanisms. These results will be helpful in the interpretation of isotope data taken from calcareous algae and other calcareous organisms grown under controlled laboratory conditions to identify isotope effects induced by environmental parameters. (2) Carbon and oxygen isotope data from marine calcareous algae will establish a database that can be used to model variation in marine $\delta^{13}C$ values. A brief discussion of the importance of algal calcification in determining the $\delta^{13}C$ value of marine DIC is provided.

2. Previous research

2.1. Algal calcification

Calcification mechanisms of Codiacean green algae are classified on the basis of microstructure of the calcification site (e.g., Wilbur et al., 1969; Bohm et al., 1978). Intercellular calcification describes the ultrastructure of calcification sites in most *Halimeda* sp. and some *Udotea* sp. specimens. Sheath calcification is known to occur in the head of *Penicillus* sp. (as filaments), *Rhipocephalus* sp. (as blades), and some *Udotea* sp. The driving mechanism of precipitation at the calcification site is often described as photosynthesis-induced pH change (e.g., Borowitzka, 1986). A close association of organic matter with the initiation of $CaCO_3$ precipitation is often reported (e.g., Wilbur et al., 1969). However, the role and character of this organic matter (in terms of calcification) are not well known.

Johansen (1981) summarized the proposed calcification mechanisms of coralline algae (i.e., the 'carbon dioxide utilization theory', the 'organic matrix theory', and the 'bicarbonate usage theory'). The carbon dioxide utilization theory requires a pH increase due to the photosynthetic removal of CO_2 and subsequent increase in the carbonate ion concentration. This theory may be inadequate as not all photosynthetic algae calcify. The organic matrix theory assumes that organic substances are the agents that concentrate the necessary ions or act as the templates on which $CaCO_3$ crystals are precipitated. The bicarbonate usage theory emphasizes the role of electrons originally stored in photosynthetic products that are later recovered by respiration (Digby, 1977). These electrons are thought to react with HCO_3^- to form CO_3^{2-}, which, in turn, increases the saturation state of the calcification site and induces precipitation of $CaCO_3$.

2.2. Isotope studies of calcareous algae

Isotopic studies of marine calcareous algae primarily have been conducted to determine the origin of carbonate mud (possibly formed by the disintegration of algal grains) in shelf carbonate environments (e.g., Lowenstam and Epstein, 1957; Gross, 1964; Keith and Weber, 1965; Gross and Tracey, 1966).

Keith and Weber (1965) observed a positive correlation between $\delta^{13}C$ and $\delta^{18}O$ values in various marine algae and corals. They interpreted this correlation as two-component mixing or the analysis of selected portions of materials that had a positive correlation between $\delta^{13}C$ and $\delta^{18}O$ values. Keith and Weber (1965) also described the significant variation in the $\delta^{13}C$ values among green and red algae and between different species of coralline algae. Wefer and Berger (1981) measured large differences in carbonate $\delta^{13}C$ and $\delta^{18}O$ values from different parts of individual plants, and distinguished environmentally induced 'response effects' from ontogeny-related 'stage effects'. The first attempt to use oxygen isotope data of algae as a paleoenvironmental indicator was conducted by Holmes (1983). He observed $\sim$ 1‰ difference between the $\delta^{18}O$ values of *Halimeda* segments in living plants and from carbonate sands in the Virgin Islands, ascribing it to the temperature increase ($\sim$ 4°C) during the Holocene in that area (for the last $\sim$ 4000 years).

2.3. Vital effects

Recent studies have described both metabolic and kinetic controls on the carbon and oxygen isotope ratios of biogenic carbonates (Swart, 1983; McConnaughey, 1989a;b, respectively). These studies present two plausible explanations of biological fractionation. Metabolic effects are related to the withdrawal (by photosynthesis) and input (by respiration) of CO_2 and subsequent change in the isotopic composition of the organism's 'internal DIC pool' which is potentially used for calcification (e.g., McConnaughey et al., 1997). This implies that isotopic equilibration is slowly achieved between the internal and external (ambient seawater) DIC pools. For photosynthetic organisms, isotopically light CO_2 molecules are preferentially fixed for the synthesis of organic matter (e.g., O'Leary, 1988) and, therefore, the internal DIC pool becomes enriched in ^{13}C. Carbonate skeletons formed by hermatypic corals (with zooxanthellae) are often enriched in ^{13}C compared to non-photosynthetic corals (e.g., Cummings and McCarty, 1982; McConnaughey, 1989a; Porter et al., 1989). Within a given specimen, high rates of photosynthesis usually correlate with higher skeletal $\delta^{13}C$ values (e.g., Wang et al., 1995).

The generally low $\delta^{13}C$ values of biogenic carbonates has led many workers to consider respiration as the primary cause of 'vital effects' (e.g., Erez, 1978; Swart, 1983; Grossman, 1987; Spero et al., 1991). It is postulated that respiratory CO_2 has lower $\delta^{13}C$ values than ambient DIC (e.g., DeNiro and Epstein, 1978; Epstein and Zeiri, 1988; McConnaughey et al., 1997), thereby decreasing the $\delta^{13}C$ values of the internal DIC pool and the carbonate skeleton that precipitates from it. However, McConnaughey et al. (1997) discount the possibility of respiration as being a major factor for carbon isotope disequilibria in calcareous animals living in aquatic environments where the ambient CO_2/O_2 ratio is relatively high. The effect of respiratory CO_2 incorporation into carbonate skeletons is significant in calcareous organisms living in terrestrial environments where the CO_2/O_2 ratio is relatively low. In general, variation in the $\delta^{13}C$ values of biogenic carbonates is thought to be related to metabolic activities (both photosynthesis and respiration). Metabolic activities are believed to be unrelated to oxygen isotope fractionation during skeletogenesis due to the rapid exchange between CO_2 and H_2O (e.g., Epstein et al., 1977; DeNiro and Epstein, 1979). This exchange is often catalyzed by the enzyme, carbonic anhydrase (e.g., Bundy, 1977; Paneth and O'Leary, 1985). Calcareous algae generally contain carbonic anhydrase and often have enhanced activities of the enzyme compared to non-calcareous algae (e.g., Graham and Smilie, 1976). However, the precise role of carbonic anhydrase in calcification is unknown.

Kinetic effects are comprised of isotope fractionations associated with the diffusion of CO_2 and with hydration and hydroxylation of CO_2. Although the diffusion of CO_2 favors isotopically light molecules, this process is thought to have little effect in the liquid phase (e.g., O'Leary, 1984). Discrimination against heavy isotopes during rapid hydroxylation of CO_2 has been described and simulated by McConnaughey (1989a,b) and Clark et al. (1992). McConnaughey (1989a,b) explained that the lower activation energy of $^{12}C^{16}O_2$ allows more rapid hydroxylation of the molecule than $^{12}C^{16}O^{18}O$ and $^{13}C^{16}O_2$. Therefore, isotopically light CO_2 molecules are preferentially hydroxylated and incorporated into carbonates. Since most biological carbonates are pre-

cipitated much faster than inorganic carbonates (e.g., Carpenter and Lohmann, 1992), their rapid precipitation prevents further equilibration between HCO_3^- and H_2O. It is notable that the depletion of ^{13}C and ^{18}O is explained by one process according to McConnaughey (1989a,b) and two separate processes according to Clark et al. (1992). Clark et al. (1992) suggested that the depletion of ^{13}C in rapidly precipitated carbonates is caused by the slower hydroxylation of $^{13}CO_2$. Depletion of ^{18}O is explained by the reaction of CO_2 with OH^- which is depleted in ^{18}O compared to H_2O ($\varepsilon^{18}O_{OH-H_2O} = \sim -40‰$). These two hypotheses explain why biotic carbonates generally have lower $\delta^{13}C$ and $\delta^{18}O$ values than those of inorganic precipitates and why biogenic carbonates often have a linear co-variation between $\delta^{13}C$ and $\delta^{18}O$ values. Kinetic fractionations (associated with hydroxylation reactions) appear to be the most viable explanation for oxygen isotope disequilibria in biotic carbonates.

Spero et al. (1997) have described a relation between ambient $[CO_3^{2-}]$ and carbonate $\delta^{13}C$ and $\delta^{18}O$ values in planktonic foraminifera. $\delta^{13}C$ and $\delta^{18}O$ values of symbiotic and non-symbiotic planktonic foraminifera decrease as $[CO_3^{2-}]$ increases, thereby producing a linear covariation (total variation of 1.5‰ for $\delta^{18}O$ and 3.9‰ for $\delta^{13}C$ over a range of $[CO_3^{2-}]$ from 75 to 774 μmol/kg). Although it is not clear whether the observed effect describes an equilibrium relation or 'vital effects', these results provide a possible explanation for stable isotope ratios observed in some biogenic carbonates.

3. Materials and methods

All of the specimens in this study are common representatives of extant calcareous algae in shallow marine environments. Where known, locations of the samples are indicated in the corresponding figures. Specimens of algae were treated with dilute sodium hypochlorite (Chlorox bleach) to remove surficial organic matter and then rinsed with de-ionized water. Microsamples of $CaCO_3$ were collected on the basis of visible morphological features and published physiological information to assess the inherent heterogeneity and systematic variation in $\delta^{13}C$ and $\delta^{18}O$ values within each specimen. Samples were milled using a Brasseler UP 20 hand engine (fitted with tungsten carbide burrs) for heavily calcified specimens or a surgical scalpel for poorly calcified specimens. Sample size was approximately 0.1–0.2 mg of $CaCO_3$. Prior to analysis, samples were roasted *in vacuo* at 200°C for aragonite and 380°C for calcite to remove volatile contaminants (e.g., Carpenter and Lohmann, 1992; Carpenter et al., 1991).

Carbonate $\delta^{18}O$ and $\delta^{13}C$ values were measured on a Finnigan delta–E gas ratio mass spectrometer equipped with an on-line carbonate extraction system and automated microvolume. Majority of the samples were reacted with three to four drops of anhydrous phosphoric acid at 75°C in individual reaction vessels. Some of the carbonate samples were dissolved in a common acid bath (equipped with a stirring mechanism) at 60°C. Isotope ratios are reported in (‰) relative to the PDB standard. Daily analyses of powdered calcite standards were conducted (NBS-18, 19, 20, and Brown Yule Marble). All standard analyses were within $\pm 0.1‰$ of accepted values. For some locations, ambient seawater samples were collected for isotope analysis ($\delta^{18}O_{water}$ and $\delta^{13}C_{DIC}$) at the time algae were collected. A discussion of these results is found in the text.

Organic carbon samples were collected by decalcifying portions of the algae with dilute HCl, rinsing with de-ionized water and drying at 40°C for 24 h. Dry samples were placed in 10 mm (OD) Pyrex tubes with ~ 1 g of cupric oxide wire and a silver vessel. Tubes were evacuated and sealed, then combusted at 550°C for 4 h to produce CO_2. CO_2 was cryogenically separated and then analyzed.

4. Results and discussion

Table 1 includes the taxonomic classification of marine calcareous algae that were analyzed for this study. Calcified structures, minerals, and suggested calcification styles are outlined in Table 2. Isotope data from all studied specimens are reported in the Appendices A and B.

4.1. Codiacean algae

There are several important carbonate producers in modern, shallow water carbonate settings within

Table 1
Taxonomy of selected specimens of calcareous algae

Division (class)	Order	Family	Subfamily	Genus/species	Subgroup
Chlorophyta (Chlorophyceae) Green Algae	Caulerpales	Codiaceae		*Halimeda incrassata* *Penicillus capitatus* *Udotea spinulosa*	Erect rhipsalian type
	Dasycladales	Dasycladaceae		*Acetabularia* sp.	
Rhodophyta (Florideophyceae) Red Algae	Cryptonemiales	Corallinaceae	Amphiroidea Corallinoideae Mastrophoroideae	*Amphiroa fragilissima* *Bossiella orbigniana* *Neogoniolithon* sp.	Articulated coralline Articulated coralline Nonarticulated coralline
	Nemalionales	Chaetangiaceae		*Galaxaura* sp.	

the Family Codiaceae (Dawes, 1981): *Halimeda* sp., *Penicillus* sp., *Udotea* sp., *Rhipocephalus* sp. (e.g., Hillis, 1991). *Halimeda* sp., *Penicillus* sp., and *Udotea* sp. are described below (Figs. 1–4, Appendix A).

4.1.1. Halimeda sp.

Due to its dominance and abundance in shallow marine environments, *Halimeda* sp. is the most studied of the calcareous algae (e.g., Hillis-Colinvaux, 1980). Each alga consists of numerous segments and a holdfast. Each segment consists of lengthwise-oriented filaments (medulla) and laterally displaced medullary filaments (cortex). The outermost part of the cortex is swollen and adhered, and as the plant grows, forms a semi-isolated intercellular space (ICS) (e.g., Wilbur et al., 1969). Precipitation of aragonite occurs in the ICS (e.g., Wilbur et al., 1969). As aragonite is precipitated extracellularly but in isolated compartments surrounded by a cell wall, calcification in *Halimeda* sp. is described as 'intercellular' (e.g., Borowitzka, 1982a). Calcification rate correlates positively with photosynthetic rate (e.g., Jensen et al., 1985; Borowitzka, 1986). Stark et al. (1969) also suggested that, to a lesser degree, respiration enhances calcification rates. Precipitation of aragonite in isolated compartments is believed to occur by photosynthetic uptake of CO_2 and subsequent pH increase in the ICS (e.g., Borowitzka and Larkum, 1977).

Table 2
Calcified structures, mineralogy and proposed calcification mechanisms of selected calcareous algae

Specimen	Location of $CaCO_3$	Mineral	Calcification mechanisms	Citation[a]
Halimeda sp.	ICS	Aragonite	Intercellular calcification	1
Udotea sp.	Sheath and ICS	Aragonite	Sheath/intercellular calcification	2
Penicillus sp.	Filaments — sheath	Aragonite	Sheath calcification	2
	Stalk — ?	Aragonite	?	3
Acetabularia sp.	Caps — extracellular	Aragonite	Extracellular calcification	4
	Cysts — extracellular	Aragonite	Extracellular calcification	5
	Stalk — extracellular	Aragonite	Extracellular calcification	4
Amphiroa sp.	Cell wall	high-Mg calcite	?	6
Bossiella sp.	Cell wall	high-Mg calcite	?	
Neogoniolithon sp.	Cell wall	high-Mg calcite	?	
Galaxaura sp.	ICS	Aragonite	Intercellular calcification (?)	7

ICS = Intercellular Space.

[a](l) Wilbur et al. (1969); (2) Bohm et al. (1978); (3) Flajs (1977a); (4) This study; (5) Marszalek (1975); (6) Cabioch and Giraud (1986); (7) Okazaki et al. (1982).

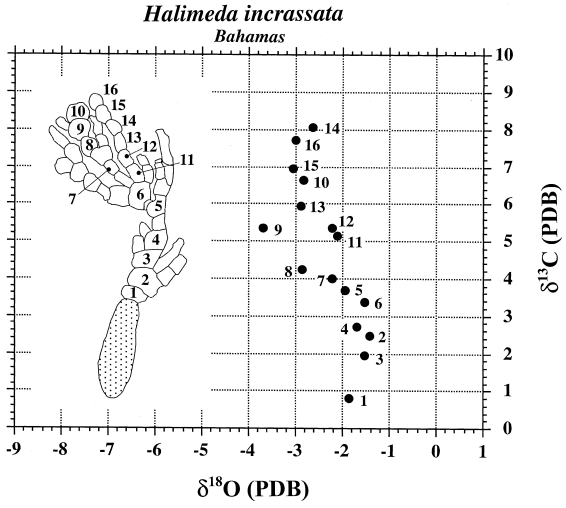

Fig. 1. $\delta^{18}O$ and $\delta^{13}C$ values of modern *H. incrassata*. Samples were taken from each numbered segment. Segments become younger and less calcified toward the top of the plant.

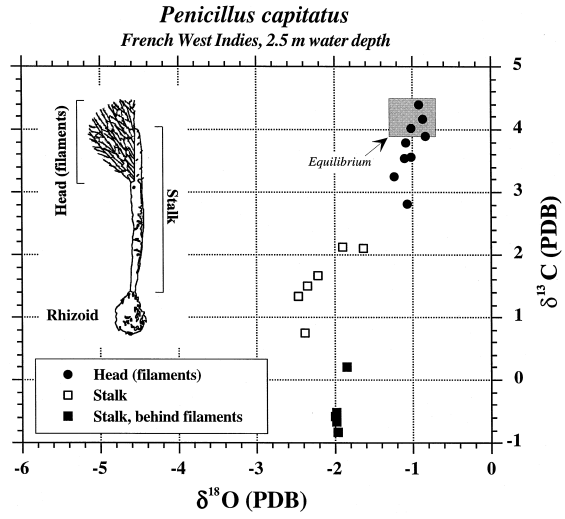

Fig. 3. $\delta^{18}O$ and $\delta^{13}C$ values of modern *P. capitatus*. The head of the plant consists of capitular filaments. Upper and lower portions of each filament were analyzed separately. Within each filament, the upper half has higher $\delta^{13}C$ and $\delta^{18}O$ values than the lower half (see Appendix A). Equilibrium aragonite $\delta^{18}O$ values were estimated using the measured $\delta^{18}O$ value of FWI seawater (0.8 ‰ SMOW at 25°C) and the fractionation factors of Friedman and O'Neil (1977) and Tarutani et al. (1969). Equilibrium aragonite $\delta^{13}C$ values were estimated using a surface water $\delta^{13}C_{DIC}$ of +1.5‰ (estimated) and the aragonite–bicarbonate enrichment factor of Romanek et al. (1992) of +2.7 ‰.

Aragonite crystals precipitated in the ICS have three different morphologies. Granular crystals are precipitated on the cell wall associated with organic matter (e.g., pilose layer of Wilbur et al., 1969). Aragonite needles grow from the granular crystals toward the center of the ICS and unbounded aggregates of aragonite needles are formed in the center of the ICS (Flajs, 1977b). These three distinct types of crystals are believed to represent the general order of calcification from the cell wall to the center of the ICS (e.g., Wilbur et al., 1969; Marszalek, 1971; Multer, 1988). In contrast, Macintyre and Reid (1995) suggest that aragonite precipitation begins in the center of the ICS as aragonite needles and granular crystals are alteration (micritization) byproducts.

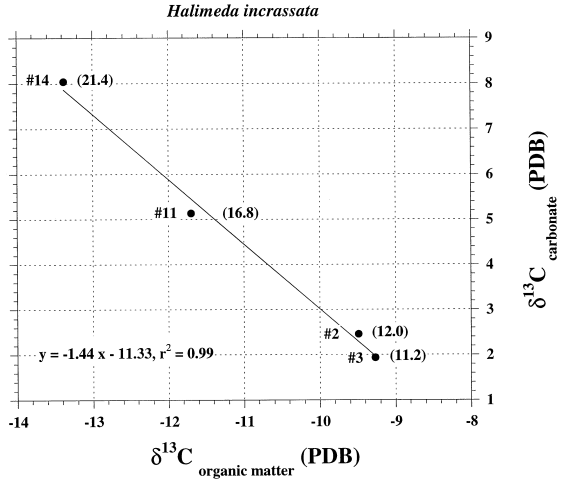

Fig. 2. $\delta^{13}C_{organic\ matter} - \delta^{13}C_{carbonate}$ values of carbonates and associated organic matter in *H. incrassata* from Fig. 1. Segment numbers corresponding to the inset in Fig. 1 are listed near each datum. Each datum indicates carbon isotope ratios of organic matter and carbonate taken from the same segment. Numbers in parentheses are the $\Delta\delta^{13}C_{Corg-Ccarb}$ for each segment analyzed.

Halimeda carbonates have a negative correlation between $\delta^{13}C$ and $\delta^{18}O$ values (Fig. 1). $\delta^{13}C$ values of younger segments are higher than the predicted equilibrium values, whereas older segments have $\delta^{13}C$ values that are lower than predicted equilibrium values. $\delta^{18}O$ values are close to the predicted equilibrium values in older segments and slightly lower (by ~1–2‰) in younger segments. Large variation in the $\delta^{13}C$ values of *Halimeda* carbonates (~7‰) can be explained on the basis of metabolic activity.

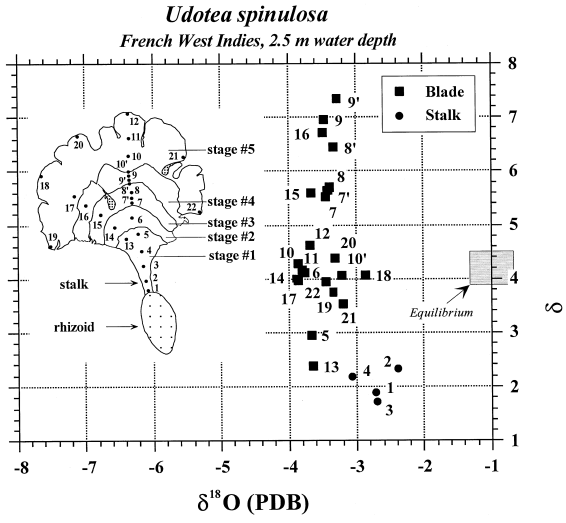

Fig. 4. $\delta^{18}O$ and $\delta^{13}C$ values of modern *U. spinulosa*. Growth stages are represented by distinct horizontal bands in the blade. Numbers and dots mark the location of isotope analyses. Equilibrium $\delta^{18}O$ and $\delta^{13}C$ values were estimated as described in Fig. 3.

There is general agreement that photosynthesis increases the $\delta^{13}C$ value of skeletal carbonate precipitated by different organisms (e.g., Cummings and McCarty, 1982; Swart, 1983; McConnaughey, 1989a). The effect of respiration also has been considered as a cause of carbon isotope disequilibrium in many calcareous organisms (e.g., Swart, 1983). Photosynthesis in the younger segments of *Halimeda* significantly enriches the associated carbonate in ^{13}C ($\delta^{13}C$ values are $\sim$3‰ higher than assumed equilibrium values). Physiologic data also confirm that this enrichment is due to enhanced photosynthesis in younger segments (485.2 nmol C fixed/min g dry weight) compared with older segments (152.8 nmol C fixed/min g dry weight) (for *H. tuna* from Borowitzka and Larkum, 1976a).

The decrease of carbonate $\delta^{13}C$ values in older segments can be linked to the incorporation of respired CO_2 into carbonates. The possibility of respiratory CO_2 use during algal carbonate precipitation can be found in the plant's physiology. *Halimeda* sp., like other calcareous algae, precipitates carbonate during the day under the influence of photosynthesis (also called light calcification) and during the night under the influence of respiration (also called dark calcification). From the physiology of the upper 11 segments of field-collected *Halimeda cylindracea* (erect rhipsalian form), dark calcification accounts for 36–46% of total calcification of the plant and generally the proportion increases as segments mature (Borowitzka and Larkum, 1976a). Incorporation of respired CO_2 is assumed to occur during dark calcification. Therefore, dark calcification rates may indicate the upper limit of respiratory CO_2 use during carbonate precipitation.

A simple mixing relation can be constructed to evaluate the extent of respiratory CO_2 input. For the upper 10 segments of *H. incrassata* studied here (segment nos. 5–16 in Fig. 1), the $\delta^{13}C$ values of organic matter range from -13.4‰ to -11.7‰ and carbonate $\delta^{13}C$ values decrease from 8.1‰ to 3.4‰. $\delta^{13}C$ values of respired CO_2 are assumed to be the same as those of organic matter and more than 90% of respired CO_2 is assumed to be hydroxylated to form HCO_3^- at physiologic pH (McConnaughey et al., 1997). Therefore, $CaCO_3$ precipitated from respired CO_2 would have $\delta^{13}C$ values ranging from -10.7‰ to -9.0‰ (using an aragonite-HCO_3^- enrichment factor $+2.7$‰; Romanek et al., 1992). For the changes of carbonate $\delta^{13}C$ values of 8.1‰ to 3.4‰, the mixing relation can be expressed as: $8.1(1-X)+(-10.7 \text{ to } -9.0)X = 3.4$, where X is the proportion of the carbonates precipitated from respiratory CO_2. The resulting value of X is $\sim$25–27%, which is slightly lower than the amount of dark calcification ($\sim$36–46%; Borowitzka and Larkum, 1976a). Although the result is a conservative estimate of respiratory carbon input, it is reasonable to assume that the decrease of carbonate $\delta^{13}C$ values is due primarily to the incorporation of respired CO_2.

The proportion of carbonate precipitated from respiratory CO_2 in basal segments of *H. incrassata* (segment nos.1–4 in Fig. 1; on the basis of the criteria of Hillis-Colinvaux, 1980) calculated using the mixing equation (described above) yields values of $\sim$40–50%. The equation of Tanaka et al. (1986) (generally used for non-photosynthetic organisms):

$$\%\,\text{metabolic carbon (M)} = \left[\delta^{13}C_{CaCO_3} - \delta^{13}C_{DIC} - \alpha_{\text{aragonite-DIC}}\right] / \left[\delta^{13}C_{\text{metabolic}} + \alpha_{\text{aragonite-CO}_2} - \delta^{13}C_{DIC} - \alpha_{\text{aragonite-DIC}}\right] \times 100,$$

produced a range of 3–20% of respiratory CO_2 input in these segments. Since detailed physiologic information of basal segments is unavailable, it is difficult to evaluate the validity of these calculations. However, characteristics of the basal segments are distinct from the other segments. (1) Unlike younger segments, which are shed off after a growth period, basal segments can survive several years and can continuously regenerate new segments (e.g., Hillis-Colinvaux, 1980). (2) The weight of $CaCO_3$ in basal segments is significantly higher than that of younger segments (up to 10 times). In nature, basal segments are generally less pigmented and, therefore, it is believed that their photosynthetic ability is significantly reduced compared to the younger segments. In addition to $CaCO_3$ being added to the ICS, it is also added to the center of the segments (medulla). Therefore, we conclude that calcification in the basal segments occurs continuously under a greater influence of respiration.

The role of respiratory CO_2 in the carbon budget of the ICS of *Halimeda* is also discussed by Borowitzka and Larkum (1976b). By labeling respiratory CO_2 with ^{14}C, they found that both calcification and photosynthesis use respiratory CO_2, and $\sim 40–50\%$ of $^{14}CO_2$ fixed by the plant is used for calcification. It is also notable that, from their experiment, input of respiratory CO_2 occurs largely during light calcification. This suggests that the amount of $CaCO_3$ precipitated from respiratory CO_2 can be larger than the amount estimated from the proportion of dark calcification.

If respired CO_2 is incorporated into skeletal carbonate and constitutes one of the major sources of carbon for calcification (due to the isolation of the calcifying compartment from ambient seawater), a systematic relation between $\delta^{13}C_{carbonate}$ and corresponding $\delta^{13}C_{organic\ matter}$ values is anticipated. This relation is observed in Fig. 2, where $\delta^{13}C$ values of carbonate and organic matter produce a negative linear correlation ($r^2 = 0.99$). Correlation of these $\delta^{13}C$ values indicates that the synthesis of organic matter (photosynthesis), the oxidation of organic matter (respiration), and calcification share a closely related carbon pool. As is illustrated in the schematic diagrams (Fig. 5A), photosynthesis, respiration, and calcification occur around the ICS in *Halimeda* sp. Photosynthesis preferentially removes $^{12}CO_2$ from the ICS fluid, leaving it enriched in ^{13}C following the formation of organic matter. As a result, $CaCO_3$ precipitated from this residual fluid has relatively high $\delta^{13}C$ values. Likewise, respiration of this organic matter releases $^{12}CO_2$ and decreases the $\delta^{13}C$ value of the ICS fluid. Therefore, $CaCO_3$ precipitated from a respiration-dominated ICS fluid has relatively low $\delta^{13}C$ values.

Fig. 2 indicates that the variation in carbonate $\delta^{13}C$ values is related to both photosynthesis and respiration, and that with a slow exchange of seawater, the ICS of *Halimeda* sp. behaves as a semi-closed system with respect to DIC. Note that the $\delta^{13}C$ values of organic matter from older segments of *H. incrassata* are up to 4‰ higher than younger segments, indicating that the $\delta^{13}C$ value of organic matter remaining after respiration is higher (e.g., DeNiro and Epstein, 1978). Also notable is the difference between $\delta^{13}C$ values of organic matter and of carbonates in each segment (Fig. 2). $\Delta^{13}C_{org\text{-}carbonate}$ is highest in segment no. 14 (younger) and lowest in no. 3 (older). The decrease in $\Delta^{13}C_{org\text{-}carbonate}$ is caused by an increase in the $\delta^{13}C$ values of organic matter and a decrease in the $\delta^{13}C$ values of carbonate as segments mature. As mentioned previously, the increase in $\delta^{13}C$ value of organic matter towards the older segments can be interpreted as the effect of respiration. The lower carbonate $\delta^{13}C$ value in the older segments can be explained by the incorporation of respiratory CO_2 into the carbonate. The combined effect of these two processes is represented as the systematic change in $\Delta^{13}C_{org\text{-}carbonates}$ (Fig. 2). This relation indicates that re-distribution of ^{12}C occurs within the ICS (via photosynthesis (production of organic matter) and calcification). ^{12}C from the ICS is used to synthesize organic matter during photosynthesis. Then, ^{12}C is released into the ICS by respiration. The semi-closed ICS retains respiratory CO_2 and this isotopically light CO_2 is incorporated into carbonates (see left portion of Fig. 5A).

McConnaughey et al. (1997) questioned the input of respiratory CO_2 into carbonate skeletons (especially for aquatic organisms) on the basis that biological membranes have high CO_2 permeabilities (e.g., Sultemeyer and Rinast, 1996). Similar uncertainty can be suggested for the role of respiration in plant calcification as plants are photosynthetic and calcifi-

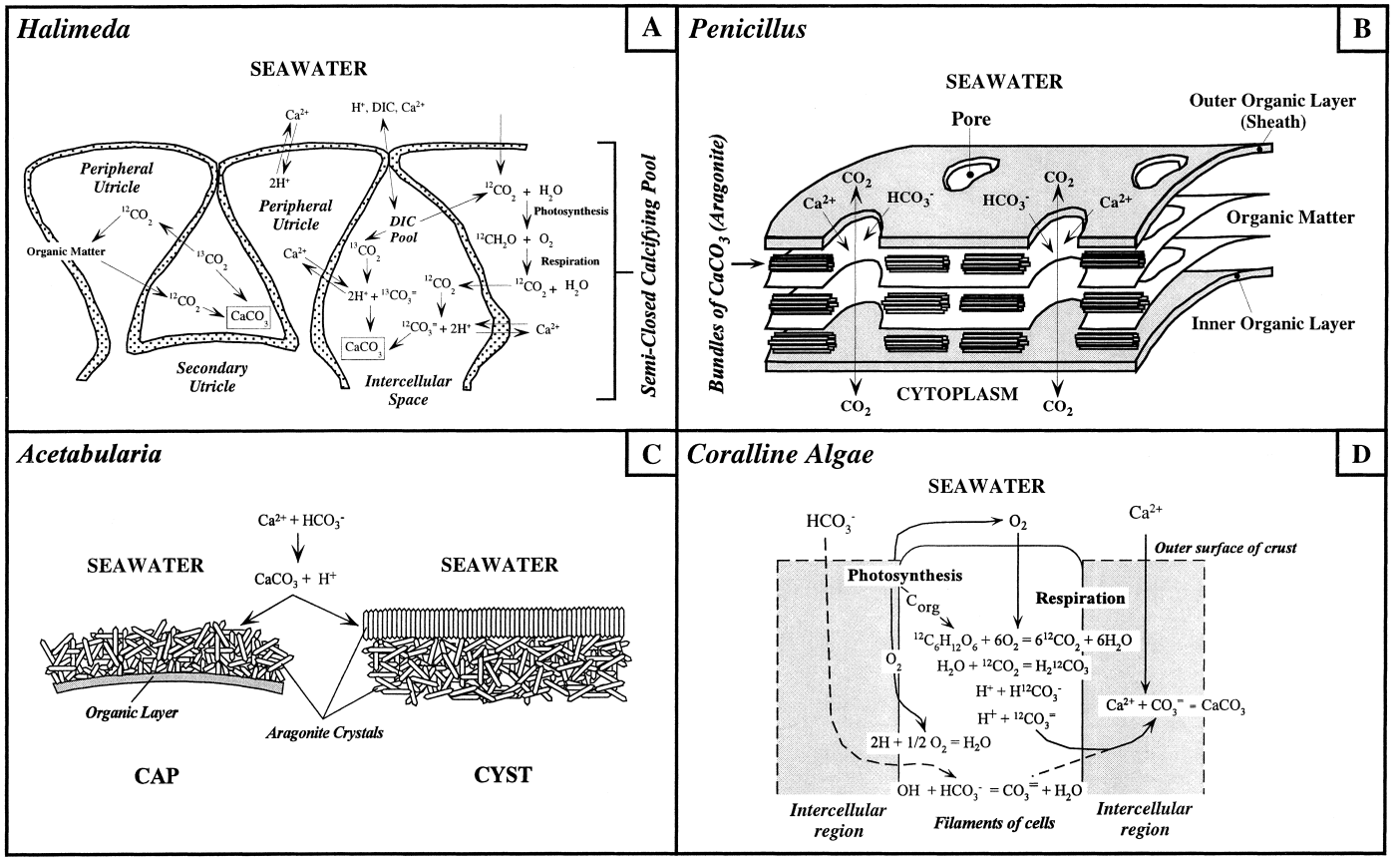

Fig. 5. (A) Schematic model of intercellular calcification in *Halimeda* and *Udotea* sp. (modified from Borowitzka, 1977). (B) Schematic model of sheath calcification in *Penicillus* sp. (drawn from information in Marszalek, 1971; Flajs, 1977a; Bohm et al., 1978). (C) Schematic model calcification in *Acetabularia* sp. (D) Schematic model calcification in coralline algae (modified from Digby, 1977).

cation is known to occur when photosynthesis rates are high (e.g., Borowitzka, 1986). The flux of ambient DIC to the calcification site, relative to the metabolic flux, determines the extent of metabolic effects on $\delta^{13}C$ value of carbonates. The ultrastructure of the calcification site influences the material exchange between ambient seawater and the calcification site. ICS in *Halimeda* sp. is semi-isolated from ambient seawater (e.g., Wilbur et al., 1969; Borowitzka and Larkum, 1977). Therefore, the $\delta^{13}C$ value of the ICS is readily modified by metabolic activities. Although the ICS is a well-described calcification site, biochemical reactions in this space are not well known (e.g., Borowitzka and Larkum, 1976b). Size of the space, characteristics of the membrane, pH, the degree of carbonic anhydrase activity, and behavior of metabolic CO_2 need to be assessed in a more quantitative way. We suggest (on the basis of isotope data and known physiologic information) that incorporation of respiratory CO_2 is important in modifying the $\delta^{13}C$ value of carbonate in *Halimeda* sp.

Variation in $\delta^{18}O$ values requires a different explanation than that outlined above as metabolic effects are thought not to affect oxygen isotope ratios (e.g., DeNiro and Epstein, 1979; Epstein et al., 1977). Given that younger *Halimeda* segments have higher calcification rates, the small depletion of ^{18}O in these segments may be caused by a kinetic fractionation associated with the hydroxylation of CO_2 (e.g., McConnaughey, 1989a,b). However, no kinetic effect (depletion of ^{13}C) is observed in the $\delta^{13}C$ values of the apical segments. An alternative explanation may be that the range of $\delta^{18}O$ values is the result of seasonal temperature variation.

It also has been suggested that early-formed aragonite crystals in *Halimeda* sp. are dissolved and re-precipitated as segments mature. Macintyre and Reid (1995) have provided petrographic evidence for the micritization of aragonite crystals during ontogeny. Bohm and Goreau (1973), using isotope labeling techniques, observed that there is an exchange of Ca^{2+} between aragonite and the labeled medium following initial calcification of *H. opuntia* segments. If abiotic re-crystallization is a common process in living *Halimeda* sp., then the $\delta^{18}O$ and $\delta^{13}C$ values of the re-crystallized portions should approach predicted equilibrium values for a given location. Our data suggest that $\delta^{13}C$ values of the oldest segment of *H. incrassata* are actually lower than predicted aragonite equilibrium values (Fig. 1). Given that ambient fluids are several times supersaturated with respect to aragonite, there is little inorganic chemical drive for aragonite dissolution. However, these reactions could be biologically mediated and unrelated to ambient saturation states.

4.1.2. Penicillus sp.

Penicillus sp. consists of a rhizoid, stalk, and capitular filaments (head) (Fig. 3). Capitular filaments are sites of photosynthesis and heavy calcification. Aragonite crystals in the filaments of *Penicillus* are precipitated in a 'sheath compartment' (Bohm et al., 1978). This sheath is an organic layer surrounding the inner organic layer that contains cytoplasm. Between these two layers, bundles of aragonite crystals are arranged subparallel to the filament axis (see Fig. 5B). This sheath compartment is three to five orders of magnitude smaller than the 'ICS' of *Halimeda* (Bohm et al., 1978). The sheath (outer layer) has numerous pores the diameters of which are $\sim 20–35$ μm and are $\sim 20–40$ μm apart from each other (e.g., Marszalek, 1971; Flajs, 1977a; Bohm et al., 1978). The pores are devoid of aragonite crystals yet appear to be important for calcification, as the exchange of solutes between ambient seawater and calcification sites is possible through the pores (see Fig. 5B). Crystal organization in the stalk is different than in the capitular filaments. Crystals adjacent to the cell wall are granular and, in the center of compartments, acicular aragonite is precipitated with a random orientation. Bundles of aragonite needles similar to those in the capitular filaments are also found in the stalk (e.g., Flajs, 1977a; Marszalek, 1971). The character of the calcifying compartment in the stalk is not clear, but it appears to be similar to that of the ICS of *Halimeda* and *Udotea*.

The capitular filaments and the stalk of *Penicillus* sp. have distinctly different $\delta^{13}C$ and $\delta^{18}O$ values (Fig. 3). Capitular filaments have relatively high $\delta^{13}C$ and $\delta^{18}O$ values that are near predicted equilibrium values. The relatively small variability in the $\delta^{18}O$ values of capitular filament carbonate ($-1‰ \pm 0.3$) is similar to that found in abiotically precipitated marine cements (e.g., Carpenter et al., 1991).

The near-equilibrium values of filaments can be explained by the unique character of the calcifying compartment (Fig. 5B). Since calcification in the filaments occurs in a relatively open environment, $\delta^{13}C$ and $\delta^{18}O$ values of the aragonite are expected to be very close to equilibrium values. The upper portions of filaments have consistently higher $\delta^{13}C$ values than those of the lower portions (see Appendix A). It is likely that this variability is the result of variable photosynthetic activity along a single filament. Similar sheath calcification is reported in a few species of *Udotea* and the blade-shaped head of *Rhipocephalus* sp. (Bohm et al., 1978). The head of *Rhipocephalus* sp. also has relatively consistent $\delta^{13}C$ and $\delta^{18}O$ values that are close to the predicted equilibrium values (Lee, unpublished data).

The stalk of *Penicillus* has $\delta^{18}O$ values that are lower than those of the filaments (~ -2‰ with little variability). Stalk $\delta^{13}C$ values are variable and lower than predicted equilibrium values (Fig. 3). Interestingly, the $\delta^{13}C$ values of the stalk behind the filaments are much lower than those areas of the stalk not covered by filaments (Fig. 3). We assumed that aragonite precipitation in this shaded area of the stalk occurs under a greater influence of respiration than the rest of the stalk. Clearly, the calcifying compartments in the stalk do not allow rapid exchange of DIC (and other solutes) with ambient seawater. The semi-isolated character of this compartment indicates similarity with those of *Halimeda* and *Udotea* sp. The SEM images of the calcified structure in the stalk of *Penicillus* sp. (e.g., Marszalek, 1971; Flajs, 1977a) are also similar to carbonates in the ICS of *Halimeda* and *Udotea*, indicating a possibility of similar calcification processes among these species.

4.1.3. Udotea sp.

Mature specimens of *Udotea* sp. consist of a rhizoid, stalk, and blade (capitulum) (Colombo, 1978; Fig. 4). The blade is the site of photosynthesis and calcification. Like *Halimeda*, the more mature growth stages are more heavily calcified. The capitulum is either cup-shaped (e.g., *U. cyathiformis*) or fan-shaped (e.g., *U. spinulosa*, *U. flabellum*). Variable calcification styles have been observed from different *Udotea* species. *U. cyathiformis* and *U. conglutinata* use sheath calcification and *U. flabellum* uses a process that is similar to intercellular calcification (Bohm et al., 1978). Morphological variation in carbonate $\delta^{13}C$ and $\delta^{18}O$ values is observed between the blade and the stalk of *U. spinulosa* (Fig. 4). Each growth stage (marked by a clearly visible band) has distinctly different $\delta^{13}C$ values. The $\delta^{13}C$ values of the stalk and blade increase toward the younger portion of the plant except for the youngest growth stage, which has significantly lower $\delta^{13}C$ values (Fig. 4). The $\delta^{18}O$ values of blade aragonite do not vary significantly (from -3.9‰ to -2.9‰) and the stalk has the highest $\delta^{18}O$ values and lowest $\delta^{13}C$ values measured in this specimen. This overall trend is similar to that observed in *H. incrassata* (Fig. 1) with the exception of the relatively low $\delta^{13}C$ values of Stage 5, suggesting that photosynthesis rates are higher in Stage 4 than in Stage 5 (Fig. 4). On the basis of the similar $\delta^{18}O$ and $\delta^{13}C$ values from *Udotea spinulosa* and *H. incrassata*, we conclude that they use similar calcification processes (Figs. 1, 4). *U. spinulosa* and *Penicillus capitatus* from the same location (French West Indies) have different $\delta^{18}O$ values (-3.9‰ to -2.4 and -2.5‰ to -0.8‰, respectively), indicating a significant difference in 'vital effects'.

Unlike the $\delta^{13}C$ values, the $\delta^{18}O$ values of Codiacean algae cannot be explained on the basis of metabolic activity. Depletion of ^{18}O (relative to the predicted equilibrium value) is relatively large in *Udotea* (~ 1.5–3‰) and small in *Penicillus* carbonates (~ 1‰) (Figs. 3, 4). Lack of a corresponding decrease in $\delta^{13}C$ values (within a given morphologic feature) argues against kinetic effects as described by McConnaughey (1989a,b) and Clark et al. (1992). However, it is possible that the fractionation of oxygen in these algae occurs via an undocumented process.

4.2. Dasycladacean (Acetabularia sp.)

Acetabularia sp. is a unicellular alga found in tropical and subtropical shallow marine settings particularly in slightly hypersaline, low-energy environments (e.g., Genot, 1991; Marszalek, 1975). Like *Halimeda*, the physiology of *Acetabularia* is also well studied (e.g., Puiseux-Dao, 1970). The typical morphology of *Acetabularia* sp. consists of rhizoid, cylindrical stalk, and reproductive cap. Radial chambers of the cap are filled with calcified cysts that

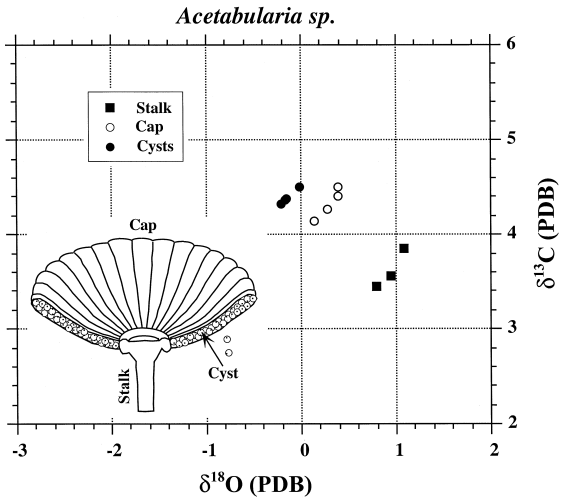

Fig. 6. $\delta^{18}O$ and $\delta^{13}C$ values of modern *Acetabularia* sp. Note that the data cluster around an assumed equilibrium value. Somewhat high $\delta^{18}O$ values indicate growth in slightly hypersaline water.

contain gametes (Fig. 6). Although the physiology of *Acetabularia* is well studied, little is known about the calcification mechanism of this alga (e.g., Borowitzka, 1982b). The hollow calcispheres (cysts) of *Acetabularia antillana* consist of acicular aragonite in the wall (~ 0.4 μm wide and ~ 7 μm long). The smooth surface of the wall, which appears polished in reflected light, is formed by the terminations of parallel acicular crystals (Marszalek, 1975). Our scanning electron microscope examinations indicate that the cap consists of thick extracellular deposits of acicular aragonite that are granular near the interior organic layer. Although poorly calcified, the stem is also covered with extracellular aragonite deposits.

The $\delta^{13}C$ and $\delta^{18}O$ values of *Acetabularia* sp. have an overall negative correlation (Fig. 6). However, each morphological component has a positive correlation with slightly different $\delta^{13}C$ and $\delta^{18}O$ values. *Acetabularia* sp. has $\delta^{13}C$ and $\delta^{18}O$ values that are very close to predicted equilibrium values. These data are consistent with the observation that aragonite are precipitated extracellularly (e.g., Marszalek, 1975). In addition, the overall variation of both $\delta^{13}C$ and $\delta^{18}O$ values is comparable with abiotically precipitated marine cements (e.g., $\pm -$ 0.3‰; Carpenter et al, 1991). The petrographic and isotopic similarities with marine cements (e.g., Land and Goreau, 1970; Ginsburg and James, 1976; Ginsburgh et al., 1971; James et al, 1976), suggest that *Acetabularia* exerts little biological influence on the calcification process (Fig. 5C).

4.3. Calcareous red algae (*Galaxaura* sp.)

Aragonite precipitation in the calcareous red alga *Galaxaura* occurs in large ICS in cortical tissue beneath the epidermal cell layer (Okazaki et al., 1982). The ICS is filled with a fibrous substance and 'electron dense particles' appear on these fibers (associated with the initiation of carbonate precipitation — presumably nuclei of $CaCO_3$). In *Galaxaura fastigiata*, crystals are typically granular (~ 0.1 μm diameter) and as calcification proceeds during maturation, they approach and even penetrate the cell wall (Okazaki et al., 1982). Flajs (1977a) observed parallel aggregates of aragonite needles between the cortical and the axial zones. Okazaki et al. (1982) proposed a relation between photosynthesis and calcification as the initiation of aragonite precipitation occurs in portions of the plant with well-developed chloroplasts.

$\delta^{13}C$ values decrease toward the younger portions although the variation is small (Fig. 7). The $\delta^{13}C$ values of *Galaxaura* sp. are as high as those of

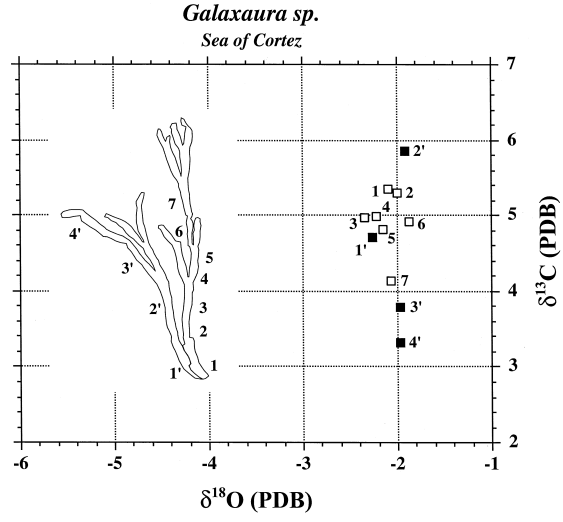

Fig. 7. $\delta^{18}O$ and $\delta^{13}C$ values of modern *Galaxaura* sp. No. 1 on each branch indicates the basal segment. Higher numbers indicate successively younger segments. Note nearly invariant $\delta^{18}O$ values.

codiaceans, yet the overall morphology-related variation is similar to articulated coralline algae. $\delta^{18}O$ values are almost invariant (ranging from $-2.3‰$ to $-1.9‰$). Like the interpretation of *Halimeda* and *Udotea*, these high $\delta^{13}C$ values are thought to be the result of photosynthesis. Interestingly, *Galaxaura* sp. has characteristics of both Codiaceans (ICS calcification, aragonite mineralogy, and high $\delta^{13}C$ values) and variation of $\delta^{13}C$ values similar to articulated coralline algae (apical segments with relatively low $\delta^{13}C$ values).

4.4. Coralline algae

Although the calcification mechanism in coralline algae is not well understood, some studies of algal ultrastructure have described calcified features (e.g., Bailey and Bisalputra, 1970; Cabioch and Giraud, 1986). Coralline algae precipitate high-Mg calcite (HMC) in the cell wall in close association with polysaccharide fibrils. Calcification occurs in two steps. In the first step, calcite needles are precipitated in the outer zone of cells, tangential to the cells and parallel to the polysaccharide fibrils. In the second step, crystals are precipitated perpendicular to the cell wall and precipitation proceeds inward. In both cases, crystals are oriented according to the direction of the polysaccharide fibrils among which they are formed (Cabioch and Giraud, 1986). Cabioch and Giraud (1986) have emphasized the importance of polysaccharide production in the calcification process as the polysaccharide fibrils act as a matrix for calcification.

The relation between calcification and metabolic activities in coralline algae has been examined by several workers (e.g., Pearse, 1972; Borowitzka, 1979; 1981). Unlike Codiaceans (green algae), these descriptions of physiology produce contradictory interpretations as both respiration (e.g., Pearse, 1972; Digby, 1977; LaVelle, 1979) and photosynthesis (e.g., Pentecost, 1978; Borowitzka, 1979, 1981) are critical processes responsible for carbonate precipitation. Biochemical reactions that directly link calcification with metabolic activities are poorly documented (e.g., Borowitzka and Larkum, 1976b; Digby, 1977). Metabolic activities may only be indirectly related to calcification as the energy-generating processes. In this case, the effect of metabolic activities on skeletal isotopic compositions is simply caused by modifying the isotopic composition of the 'internal DIC pool' (McConnaughey et al., 1997). It is known that the growth rate of coralline algae is slow and a large part of the energy is believed to be used for skeletogenesis (Digby, 1977).

4.4.1. Amphiroa sp.

The $\delta^{13}C$ values of *Amphiroa* sp. are significantly lower than those of Codiacean algae (by a maximum of 14‰). Although the Codiaceans are composed of aragonite and the coralline algae of HMC, the mineralogy-dependent carbon isotope fractionation accounts for approximately 1.7‰ of the difference between these two groups (e.g., Romanek et al., 1992). Unlike *Halimeda* and *Udotea* sp., the younger portion of the plant has lower $\delta^{13}C$ values and the older portion has higher $\delta^{13}C$ values. The $\delta^{18}O$ values of *Amphiroa* sp. are relatively invariant (individual branches have less than 0.6‰ variation) and are lower than predicted equilibrium values by $\sim 3.5‰$.

The low $\delta^{13}C$ and $\delta^{18}O$ values of *Amphiroa* carbonate are not consistent with the kinetic fractionations observed during hydroxylation of CO_2 (i.e., there is no linear co-variation of $\delta^{13}C$ and $\delta^{18}O$ values, McConnaughey, 1989a,b; Clark et al., 1992; Fig. 8). Metabolic activities associated with kinetic fractionations may modify this co-variation. Highly photosynthetic portions of *Acropora palmata* have higher $\delta^{13}C$ values than low photosynthetic portions, yet have a similar range of $\delta^{18}O$ values. This produces two parallel trends offset by $\sim 2‰$ in $\delta^{13}C$ values (Wang et al., 1995). McConnaughey (1989a) also noted the similar type of relation in the isotope data of hermatypic and ahermatypic corals that produces two linear arrays with different slopes. Both respiration and kinetic fractionations lower $\delta^{13}C$ values in carbonates. The combined effects of respiration and kinetic fractionations should result in a co-variation between $\delta^{13}C$ and $\delta^{18}O$ values with a steeper slope than via kinetic fractionation alone (e.g., *Acropora cervicornis* of Wang et al., 1995). The high pH (as high as 10) in the calcifying sites of many calcareous algae and the direct exchange between CO_2 and $CO_3^=$ may be considered as a reason

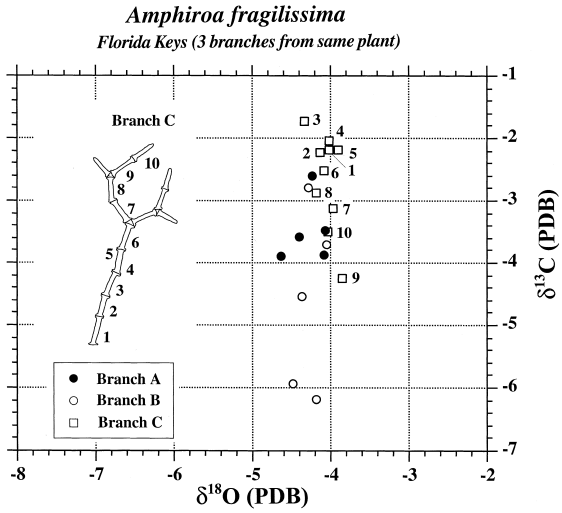

Fig. 8. $\delta^{18}O$ and $\delta^{13}C$ values of modern *Amphiroa* sp. For simplicity, only branch no. 3 is shown in the inset figure. About 1/3 of each intergenicula was used for analysis. Each datum represents one intergenicula (except nos. 4 and 5 that are from same intergenicula). $\delta^{13}C$ values decrease toward younger portion of each branch. Note that each branch has less than 0.6‰ total variation in $\delta^{18}O$ values.

for the lack of co-variation (McConnaughey, personal communication). However, empirical data and laboratory simulations of kinetic effects at high pH still produce linear co-variation between carbon and oxygen isotope ratios (Clark et al., 1992). The lack of co-variation between $\delta^{13}C$ and $\delta^{18}O$ values in *Amphiroa* carbonate argues against kinetic fractionations (or at least kinetic fractionation processes currently understood) as a means of producing these values.

Most articulated coralline algae do not have chloroplasts in their apical tips (e.g., Pearse, 1972; LaVelle, 1979). Apical tips grow mostly by translocation of organic matter from more mature portions of the plant and, therefore, calcification in the apical segment occurs under the strong influence of respiration. Unlike Codiaceans, photosynthetic effects are greater in the older intergenicula of coralline algae. $\delta^{13}C$ values are expected to be lower in apical intergenicula (due to stronger effects of respiration) and higher in older portions of the plant (due to stronger effects of photosynthesis). Variation of *Amphiroa* carbonate $\delta^{13}C$ values is in agreement with these physiologic data (Fig. 8). Approximately 36–56% of calcification in *Amphiroa* sp. occurs without light (Borowitzka, 1979). The $\delta^{13}C$ value of organic matter from the *Amphiroa* specimen studied here is −21.5‰. Using the equation of Tanaka et al. (1986), the proportion of respiratory CO_2 in *Amphiroa* carbonates ranges from 16% (in old intergenicula) to 36% (in young intergenicula). Therefore, carbon isotope disequilibrium in *Amphiroa* carbonates can be explained by metabolic effects. Individual branches of *Amphiroa* sp. have less than 0.6‰ variation in $\delta^{18}O$ values (Fig. 8), which is similar to the variation observed in modern, abiotically precipitated marine cements (e.g., Gonzalez and Lohmann, 1985; Carpenter et al., 1991). As *Amphiroa* is consistently lower (by ~3.5‰) than predicted equilibrium $\delta^{18}O$ values, it may provide a useful seawater proxy.

4.4.2. *Bossiella sp.*

Bossiella orbigniana, another articulated coralline alga, has $\delta^{13}C$ values that are similar to those of *Amphiroa* sp. (both composed of HMC; Fig. 9). $\delta^{13}C$ values decrease by approximately 2.5‰, whereas $\delta^{18}O$ values decrease by approximately 1‰ toward the younger portion of the plant (Fig. 9). $\delta^{13}C$ and $\delta^{18}O$ values co-vary with a slope of +2.2 (r^2 = 0.60). The covariance of $\delta^{13}C$ and $\delta^{18}O$ values in *B.*

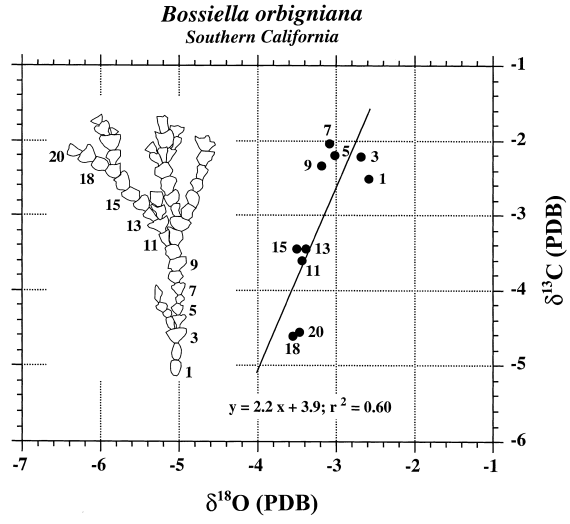

Fig. 9. $\delta^{18}O$ and $\delta^{13}C$ values of modern *B. orbigniana*. No. 1 is the basal intergenicula and no. 20 is the apical intergenicula.

orbigniana carbonate suggests that kinetic fractionation of carbon and oxygen during hydroxylation of CO_2 affects these values. However, it is assumed that, on the basis of a common physiology among articulated coralline algae, respiration also plays a role in the carbon isotope disequilibria of this species (e.g., Pearse, 1972). Confirmation of such kinetic effects may be possible by direct precipitation rate measurements or by analysis of precipitation rate-dependent cation concentrations (e.g., Lorens, 1981; Carpenter and Lohmann, 1992).

4.4.3. *Neogoniolithon sp.*

A positive, linear correlation between $\delta^{13}C$ and $\delta^{18}O$ values is observed in the nonarticulated coralline alga *Neogoniolithon* sp. (slope $= +1.6$, $r^2 = 0.64$; Fig. 10). These data are similar to those of many other calcareous organisms (e.g., Keith and Weber, 1965; Weber and Raup, 1966a,b; Swart, 1983; Carpenter and Lohmann, 1995). $\delta^{13}C$ and $\delta^{18}O$ values are not correlated with sample locations (that cover the entire length of the specimen). To examine possible ontogenetic and microarchitectural variations in isotopic ratios, a different sampling strategy should be applied to this species since the stems of the alga grow radially as well as vertically (e.g., Moberly, 1968).

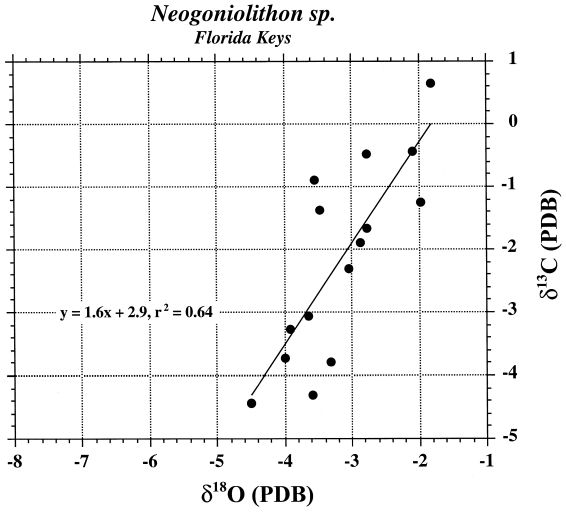

Fig. 10. $\delta^{18}O$ and $\delta^{13}C$ values of modern *Neogoniolithon* sp. Samples were taken along a traverse from the lower to upper end of the plant. No relation between sample location and isotopic composition is found.

We conclude that the significant difference in $\delta^{13}C$ values between coralline algae and Codiacean green algae is the result of different physiology associated with calcification. From the simple calculations for *Halimeda* and *Amphiroa* carbonates, the proportion of carbonate precipitated from respiratory CO_2 is not significantly different ($\sim$25–27% for *Halimeda* and $\sim$16–36% for *Amphiroa*). The difference in $\delta^{13}C$ values in these calcareous algae appears to be related to the difference in $\delta^{13}C$ values of organic matter (from -13.4‰ to -9.3‰ for *Halimeda* and -21.5‰ for *Amphiroa*) which controls the carbon isotope ratios of respiratory CO_2. Moreover, active precipitation of carbonates in younger portions of plants occurs under the strong influence of respiration in coralline algae and under the influence of photosynthesis in Codiaceans.

4.5. *Vital effects in marine calcareous algae*

On the basis of the microstructure, physiology and isotopic composition of $CaCO_3$, schematic diagrams for algal calcification are shown in Fig. 5. The schematic models suggested by Borowitzka (1977) and Digby (1977) are somewhat difficult to reconcile with the stable isotope data presented here for Codiacean and coralline algae (Fig. 5A,D). As a result, we have modified these calcification models. In intercellular calcification, ambient DIC does not play a direct role in determining the $\delta^{13}C$ value of algal carbonate (Fig. 5A) due to the isolation of the compartments from ambient seawater. In *Halimeda* sp., $\sim$70% of the outer cell surface is facing ICS (Borowitzka and Larkum, 1976b). Therefore, the ICS (average volume is $\sim 4 \times 10^6$ μm^3 from Bohm et al., 1978) acts as the storage of carbon for photosynthesis and calcification. Significant variation of $\delta^{13}C$ values (associated with the effects of both photosynthesis and respiration) is a distinct characteristic of this type of calcification. For the effect of respiration, a more detailed discussion about the chemical conditions at the calcification site is necessary. Release of CO_2 will decrease the pH of the calcification site and lower the saturation state with respect to $CaCO_3$. Active transport of Ca^{2+} in exchange for $2H^+$ may prevent pH decrease at the

calcification site (e.g., McConnaughey, 1989c). It is clear that additional study is required to clarify the physico-chemical condition of the calcification site. Sheath calcification (Fig. 5B) and extracellular calcification (Fig. 5C) produce $CaCO_3$ deposits whose isotope compositions are close to the predicted equilibrium values. This is due to the rapid exchange of H_2O and solutes between seawater and calcification site. For *Acetabularia* sp. (extracellular calcification), calcification appears to occur in an open space without evidence of modifying saturation state. The cause of the rapid calcification in *Acetabularia* sp. is a topic for future research.

On the basis of generally low $\delta^{13}C$ values, calcification must be related to respiration, and to a lesser extent, photosynthesis for coralline algae (Fig. 5D). Kinetic effects may explain the isotope data of *Bossiella* sp. and *Neogoniolithon* sp. (Figs. 9, 10). However, the $\delta^{18}O$ values of *Amphiroa* carbonate are not explained by the kinetic effects currently proposed by McConnaughey (1989a,b) and Clark et al. (1992). The relatively large offset from predicted equilibrium $\delta^{18}O$ and $\delta^{13}C$ values of *Amphiroa* carbonate may represent a consistent kinetic fractionation with no linear co-variation (e.g., McConnaughey, 1989a,b). The commonly observed linear co-variation between $\delta^{13}C$ and $\delta^{18}O$ values associated with kinetic fractionation is caused by re-equilibration of the hydroxylated species with ambient fluids to varying degrees (e.g., McConnaughey, 1989b). Therefore, the lack of co-variation in $\delta^{13}C$ and $\delta^{18}O$ values of *Amphiroa* carbonate may simply indicate lack of re-equilibration or a constant degree of re-equilibration with ambient fluids. It is assumed that, during calcification, consistent kinetic effects (which can be related to a constant rate of hydroxylation throughout an individual specimen or the entire *Amphiroa* sp.) fractionate both carbon and oxygen isotopes without re-equilibration with ambient DIC and H_2O (or at a constant degree of re-equilibration). $\delta^{13}C$ values are further affected by metabolic activities and may superimpose this variation on the kinetic fractionation. Given that these are non-equilibrium processes and factors such as ontogeny and variable growth rate and ambient conditions, one assumes that these conditions would yield variable isotopic compositions. However, *Amphiroa* sp. may have an ability to maintain favorable internal conditions (saturation state, pH, $[CO_3^{2-}]$, etc.) for growth and calcification despite potentially unfavorable ambient conditions. If *Amphiroa* sp. precipitates $CaCO_3$ under conditions that are biologically maintained by the organism, a consistent kinetic fractionation may be possible. If so, we are unfamiliar with these processes.

In this context, it is notable that *Amphiroa* sp. (and other coralline algae) generally has unusually low organic matter $\delta^{13}C$ values. This indicates a more efficient use of CO_2 for photosynthesis compared with other aquatic plants (e.g., Codiaceans and calcareous red algae; Lee, unpublished data). Unusually successful growth of *Amphiroa* sp. in the Biosphere 2 Ocean system (under elevated pCO_2 levels, variable saturation states, and low light levels) may be explained by the *Amphiroa*'s ability to establish favorable growth conditions. However, data from *Amphiroa* sp. grown in the Biosphere 2 ocean system (under elevated pCO_2 levels and therefore with lower $\delta^{13}C_{\text{organic matter}}$ values) indicate that there is a positive linear relation between the $\delta^{13}C$ values of carbonate and associated organic matter (Carpenter et al., 1997; Lee et al., 1997). This relation argues for use of respiratory CO_2 during calcification. It has not been determined whether the metabolic effects of respiration are superimposed on kinetic fractionations. The relatively invariant $\delta^{18}O$ values of *Amphiroa* seem to be inconsistent with our present understanding of kinetic fractionations (McConnaughey, 1989a,b; Clark et al., 1992). A more detailed examination of *Amphiroa* calcification is warranted.

The small variation in the $\delta^{18}O$ values of many calcareous algae suggests that they could be used as proxy indicators of ancient seawater (e.g., Holmes, 1983). Although most modern forms of calcareous algae are generally poorly preserved in Pleistocene age rocks, the small variation in $\delta^{18}O$ values of *Acetabularia* sp., *Amphiroa* sp. and *Galaxaura* sp. holds much promise as indicators of temperature or seawater $\delta^{18}O$ values. However, the role that 'vital effects' play in determining the $\delta^{18}O$ values of biotic carbonates is not clearly understood. The relation between extension rates, precipitation rates, $\delta^{18}O$ values and Sr^{2+}, Cd^{2+} concentrations of biotic carbonates may provide a better understanding of how kinetic isotope effects are related to calcification

rates (e.g., Lorens, 1981; McConnaughey, 1989a,b; Carpenter and Lohmann, 1992; de Villiers et al., 1994).

4.6. Algal calcification and the $\delta^{13}C$ value of marine DIC

Glacio-eustatic changes in the marine $\delta^{13}C_{DIC}$ value are currently ascribed to variable rates of preservation and destruction of organic carbon (e.g., Shackleton, 1977; Broecker, 1982) and changes in ocean circulation patterns (e.g., Curry et al., 1988). In general, marine $\delta^{13}C_{DIC}$ values (as measured in foraminiferal carbonate) are known to be lower during glacial periods (e.g., Shackleton, 1977). In part, glacial–interglacial changes in the $\delta^{13}C$ value of marine DIC can be explained by the variable size of the organic carbon reservoir (e.g., Ku and Luo, 1992). Spero et al. (1997) also have suggested that the $\delta^{13}C$ values of foraminiferal calcite are a function of $[CO_3^{2-}]$ due to variation in atmospheric pCO_2 (increased $[CO_3^{2-}]$ yields decreased $\delta^{13}C_{calcite}$ values). However, there are still uncertainties in the attempts to describe the evolution of the $\delta^{13}C$ value of marine DIC on the basis of the possible variations in the relative size of organic carbon reservoirs and the changes in ocean circulation pattern. Considering the complex nature of the carbon cycle in the marine environment, it is clear that the effects of all possible processes need to be examined in a more quantitative way.

Despite its dominance in shallow marine environments, algal calcification (and dissolution) has received little attention for its impact on the global carbon cycle (e.g., Schlanger, 1988; Opdyke and Walker, 1992). Deposition of calcium carbonate by marine algae (in both shallow shelf and deep-sea environments) is an important aspect of the global carbon cycle (e.g., Hillis-Colinvaux, 1980; Toomey and Nitecki, 1985; Patterson and Walter, 1994; Walker and Opdyke, 1995). Calcareous algae and scleractinian corals account for nearly all shallow marine carbonate production (e.g., Milliman, 1974, 1993; Schlanger, 1988). Among the calcareous algae, carbonate production by Codiaceans is significant in shallower portions of reefs and carbonate banks (e.g., Milliman, 1974; Multer, 1988; Hillis, 1991). Because most Codiaceans occur in shallow reefal settings, their production rate is directly affected by glacio-eustatic sea level changes (e.g., Hillis-Colinvaux, 1980; Hillis, 1991). As Codiacean algae predominantly occur in shallow, backreef environments and coralline algae and corals occur in reef and forereef environments, high sea level will favor Codiacean production (via an increase in shallow shelf areas) relative to corals and coralline algae. Conversely, low sea level will generally decrease Codiacean production. The disparate $\delta^{13}C$ values of Codiacean ($\delta^{13}C$ value of $\sim +4‰$) and coralline algae (and scleractinian corals; $\delta^{13}C$ value of $\sim -3‰$) carbonate (Fig. 11) suggest that a modification of shallow marine carbonate production (i.e., shifts between Codiacean and coralline algae dominance caused by a global sea level change) may affect the $\delta^{13}C$ value of marine DIC.

The flux of carbon to shallow marine carbonate has been estimated to be $1.8–2.3 \times 10^{13}$ mol/year (e.g., Opdyke and Walker, 1992) and $1.2–1.3 \times 10^{13}$ mol/year for the flux to deep-sea carbonate (e.g., Milliman, 1974; Davies and Worseley, 1981). The percentage of shallow marine carbonates composed of corals and coralline algae is $\sim 50–55\%$ (estimated from data in Kinsey and Hopley, 1991) and Codiacean green algae is $\sim 35–40\%$ (estimated from

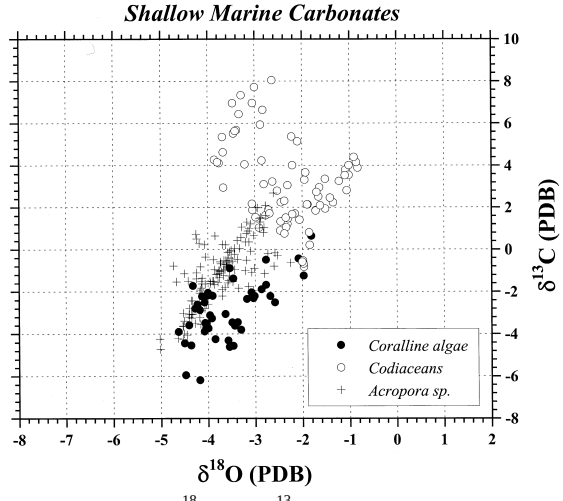

Fig. 11. Carbonate $\delta^{18}O$ and $\delta^{13}C$ values for the major $CaCO_3$ producers in tropical, shallow marine environments. Isotope data of Codiaceans and coralline algae are from this study. Isotope data for hermatypic corals (*Acropora palmata* and *Acropora cervicornis*) are from Wang et al. (1995). Note the large difference in $\delta^{13}C$ values between Codiaceans and coral/coralline algae.

data in Kinsey and Hopley, 1991). If we assume that shelf carbonates contain 40% Codiacean algae, 50% corals/coralline algae, and 10% other biogenic carbonate such as molluscs, echinoderms, and bryozoans (with a $\delta^{13}C$ value of $\sim 0‰$), then the composition of modern, shallow marine carbonates is approximately $+0.1‰$. Similarly, an average $\delta^{13}C$ value for deep-sea carbonates (a mixture of planktonic and benthonic foraminifera and calcareous nanofossils) is estimated to be $+1.5‰$.

Using these estimates together with a shallow marine carbonate flux of 2.0×10^{13} mol C/year and the deep-sea carbonate flux of 1.2×10^{13} mol C/year, a riverine carbon flux of 3.2×10^{13} mol C/year ($\delta^{13}C$ value of $\sim -4‰$; Drever et al., 1988; Carpenter and Lohmann, 1997) and an organic carbon flux of 6.6×10^{13} mol C/year ($\delta^{13}C$ value of $\sim -25‰$; Carpenter and Lohmann, 1997 and references contained within), it is possible to model the effects of glacio-eustatic sea level change on the $\delta^{13}C$ value of marine DIC. A quantitative model relating sea level changes and algal production for steady state and non-steady state conditions is being developed and will be the focus of a future publication.

5. Conclusions

'Vital effects' observed in $\delta^{13}C$ and $\delta^{18}O$ values of algal carbonates are related to ontogeny, calcification styles (i.e., intercellular, sheath compartments, extracellular), the P/R ratio associated with the specific morphologic unit of the individual alga, and involvement of kinetic processes. An understanding of the microenvironment of the calcification site is critical in understanding 'vital effects' in calcareous algae. Variation in carbonate $\delta^{13}C$ values (a maximum range of $\sim 14‰$) is produced by the relative contribution of carbon used for carbonate precipitation from ambient marine DIC, photosynthesis-modified fluids, and respiration-modified fluids. Therefore, $\delta^{13}C$ values can be much higher or much lower than predicted equilibrium values. $\delta^{18}O$ values are relatively invariant within a given specimen and, with the exception of *Amphiroa* and *Neogoniolithon* sp., are near predicted equilibrium values.

Using current carbonate production rates and $\delta^{13}C$ values, shallow marine carbonates play a significant role in controlling the change in the $\delta^{13}C$ value of marine DIC. This effect is directly related to sea-level-induced changes in the production rate of different types of shallow marine carbonates (e.g., coralline vs. Codiacean algae). The distinct $\delta^{13}C$ values of Codiacean algae and their variable carbonate production rates associated with glacio-eustatic sea level changes need to be considered when modeling short-term variation in the global carbon system.

Acknowledgements

This research was funded by Texas Advanced Research Program grant no. 009741-064 and a grant from Columbia University/Biosphere 2 Center to S.J.C. The quality of this manuscript was greatly improved by discussions with T. McConnaughey, A. Longinelli, and an anonymous reviewer. Some of the samples used in this study were provided by H. Montgomery and R. Mitterer.

Appendix A. Carbon and oxygen isotope data from algal carbonate

Description	$\delta^{13}C$ (PDB)	$\delta^{13}O$ (PDB)
Halimeda incrassata		
Segment no. 1, basal	0.80	−1.86
Segment no. 2	2.46	−1.42
Segment no. 3	1.94	−1.52
Segment no. 4	2.73	−1.70
Segment no. 5	3.67	−1.94
Segment no. 6	3.36	−1.52
Segment no. 7	4.01	−2.21
Segment no. 8	4.24	−2.86
Segment no. 9	5.35	−3.69
Segment no. 10, apical	6.64	−2.83
Segment no. 11	5.14	−2.10
Segment no. 12	5.37	−2.22
Segment no. 13	5.94	−2.88
Segment no. 14	8.05	−2.64
Segment no. 15	6.96	−3.05
Segment no. 16, apical	7.72	−3.00

Udotea spinulosa

Stalk	1.89	−2.72
Stalk	2.31	−2.38
Stalk	1.71	−2.70
Boundary between stalk and blade	2.17	−3.06
Blade, 1st growth stage	2.95	−3.67
Blade, 2nd growth stage	4.12	−3.77
Blade, 3rd growth stage	5.52	−3.46
Blade, 3rd growth stage	5.63	−3.42
Blade, 3rd growth stage	5.68	−3.39
Blade, 4th growth stage	6.44	−3.33
Blade, 4th growth stage	7.33	−3.29
Blade, 4th growth stage	6.96	−3.47
Blade, last growth stage	4.06	−3.21
Blade, last growth stage	4.28	−3.86
Blade, last growth stage	4.16	−3.80
Tip of the blade, last growth stage 'different cross section'	4.63	−3.68
Blade, 1st growth stage	2.37	−3.65
Blade, 2nd growth stage	4.00	−3.88
Blade, 3rd growth stage	5.59	−3.66
Blade, 4th growth stage	6.70	−3.49
Blade, the last growth stage	3.95	−3.85
Tip of the blade, last growth stage	4.06	−2.87
Tip of the blade, last growth stage	3.75	−3.34
Tip of the blade, last growth stage	4.39	−3.32
Tip of the blade, last growth stage	3.53	−3.19
Tip of the blade, last growth stage	3.94	−3.46

Bossiella orbigniana

1st intergenicula	−2.51	−2.59
3rd intergenicula	−2.21	−2.68
5th intergenicula	−2.20	−3.02
7th intergenicula	−2.03	−3.08
9th intergenicula	−2.34	−3.18
11th intergenicula	−3.60	−3.44
13th intergenicula	−3.44	−3.38
15th intergenicula	−3.45	−3.49
18th intergenicula	−4.61	−3.55
20th intergenicula	−4.56	−3.47

Galaxaura sp.

1st segment, basal, branch 1	5.35	−2.10
2nd segment, branch 1	5.31	−1.99
3rd segment, branch 1	4.97	−2.34
4th segment, branch 1	5.00	−2.22
5th segment, branch 1	4.82	−2.16
6th segment, branch 1	4.92	−1.88
7th segment, branch 1	4.13	−2.06
Bottom of branch 2	4.71	−2.26
1/4 of branch 2	5.85	−1.92
3/4 of branch 2	3.78	−1.98
Top of branch 2	3.32	−1.97

Penicillus capitatus

Stalk	2.14	−1.90
Stalk	0.75	−2.38
Stalk	1.33	−2.46
Stalk	1.51	−2.35
Stalk	1.68	−2.21
Stalk	2.10	−1.63
Capitular filament	3.80	−1.09
Capitular filament	3.56	−1.02
Capitular filament	3.90	−0.83
Filament, lower half	2.81	−1.06
Filament, upper half	4.16	−0.86
Filament, lower half	3.54	−1.10
Filament, upper half	4.40	−0.91
Filament, lower half	3.26	−1.23
Filament, upper half	4.02	−1.02
Stalk, behind filaments	0.22	−1.85
Stalk, behind filaments	−0.53	−1.99
Stalk, behind filaments	−0.83	−1.97
Stalk, behind filaments	−0.68	−1.98
Stalk, behind filaments	−0.59	−2.00

Acetabularia sp.

Stalk	3.56	0.95
Stalk	3.45	0.80
Stalk	3.85	1.08
Cap	4.14	0.14
Cap	4.27	0.28
Cap	4.40	0.39
Cap	4.50	0.39
Cysts	4.50	−1.01
Cysts	4.38	−0.15
Cysts	4.36	−0.17
Cysts	4.32	−0.21

Amphiroa fragilissima

1st intergenicula of branch 1, basal	−3.88	−4.08
2nd intergenicula	−3.48	−4.07
3rd intergenicula	−2.60	−4.23
4th intergenicula	−3.58	−4.41
5th intergenicula of branch 1, apical	−3.90	−4.63
1st intergenicula of branch 2, basal	−3.71	−4.05
2nd intergenicula	−2.80	−4.28
3rd intergenicula	−4.54	−4.36
4th intergenicula	−5.94	−4.48
5th intergenicula of branch 2, apical	−6.18	−4.18
1st intergenicula of branch 3, basal	−2.19	−4.02
2nd intergenicula	−2.22	−4.13
3rd intergenicula	−1.72	−4.33
4th intergenicula, lower half	−2.05	−4.01
4th intergenicula, upper half	−2.19	−3.91
5th intergenicula	−2.51	−4.08
6th intergenicula	−3.12	−3.97
7th intergenicula	−2.87	−4.18
8th intergenicula	−4.24	−3.85
9th intergenicula of branch 3, apical	−3.50	−4.03

Neogoniolithon sp.

Bottom of branch 1	−0.89	−3.54
1/4 of branch 1	−3.05	−3.64
1/2 of branch 1	0.64	−1.82
3/4 of branch 1	−3.73	−4.00
Top of branch 1	−1.36	−3.47
Bottom of branch 2	−4.44	−4.50
2/7 of branch 2	−0.49	−2.77
3/7 of branch 2	−1.67	−2.77
4/7 of branch 2	−2.31	−3.04
5/7 of branch 2	−4.30	−3.58
6/7 of branch 2	−0.43	−2.08
Top of branch 2	−3.26	−3.92
Bottom of branch 2′	−1.89	−2.87
Middle of branch 2′	−1.24	−1.98
Top of branch 2′	−3.80	−3.30

Appendix B. Carbon isotope data of organic matter

Description	$\delta^{13}C_{org}$ (PDB)
H. incrassta (segment no. 2)	−9.5
H. incrassta (segment no. 3)	−9.3
H. incrassta (segment no. 11)	−11.7
H. incrassta (segment no. 14)	−13.4
Am. fragilssima (whole specimen)	−21.5

References

Bailey, A., Bisalputra, T., 1970. A preliminary account of the application of thin sectioning, freeze etching, and scanning electron microscopy to the study of coralline algae. Phycologia 9 (1), 83–101.

Bohm, E.L., Goreau, T.F., 1973. Rates of turnover and net accretion of calcium and the role of calcium binding polysaccharides during calcification in the calcareous alga, *Halimeda opuntia* (L). Int. Rev. Gesamten Hydrobiol. 58, 723–740.

Bohm, L., Futterer, D., Kaminski, E., 1978. Algal calcification in some Codiaceae (Chlorophyta): ultrastructure and location of skeletal deposits. J. Phycol. 14, 486–493.

Borowitzka, M.A., 1977. Algal calcification. Oceanography and marine biology. Annu. Rev. 15, 189–223.

Borowitzka, M.A., 1979. Calcium exchange and measurement of calcification rates in the calcareous coralline red alga, *Amphiroa foliacea*. Mar. Biol. 50, 339–347.

Borowitzka, M.A., 1981. Photosynthesis and calcification in the articulated coralline red algae, *Amphiroa anceps* and *A. foliacea*. Mar. Biol. 62, 17–23.

Borowitzka, M.A., 1982a. Mechanisms in algal calcification. Prog. Phycol. Res. 1, 137–177.

Borowitzka, M.A., 1982b. Morphological and cytological aspects of algal calcification. Int. Rev. Cytol. 74, 127–162.

Borowitzka, M.A., 1986. Physiology and biochemistry of calcification in the Chlorophyceae. In: Leadbeater, B.S.C., Riding, R. (Eds.), Biomineralization in Lower Plants and Animals, vol. 31. The Systematics Association, Clarendon Press, Oxford, England, pp. 107–124.

Borowitzka, M.A., Larkum, W.D., 1976a. Calcification in the green alga, *Halimeda*: II. The exchange of Ca^{2+} and the occurrence of age gradients in calcification and photosynthesis. J. Exp. Bot. 27, 864–878.

Borowitzka, M.A., Larkum, W.D., 1976b. Calcification in the green alga, *Halimeda*: III. The sources of inorganic carbon for photosynthesis and calcification and a model of the mechanism of calcification. J. Exp. Bot. 27, 879–893.

Borowitzka, M.A., Larkum, W.D., 1977. Calcification in the green alga, *Halimeda*: I. An ultrastructure study of thallus development. J. Phycol. 1, 6–16.

Broecker, W.S., 1982. Ocean chemistry during glacial time. Geochim. Cosmochim. Acta 46, 1689–1705.

Bundy, H.F., 1977. Carbonic anhydrase. Comp. Biochem. Physiol., Part B 57, 1–7.

Cabioch, J., Giraud, G., 1986. Structural aspects of biomineralization in the coralline algae (calcified Rhodophyceae). In: Leadbeater, B.S.C., Riding, R. (Eds.), Biomineralization in Lower Plants and Animals, vol. 31. The Systematics Association, Clarendon Press, Oxford, England, pp. 141–156.

Carpenter, S.J., Lohmann, K.C., 1992. Sr/Mg ratios of modern marine calcite: empirical indicators of ocean chemistry and precipitation rate. Geochim. Cosmochim. Acta 56, 1837–1849.

Carpenter, S.J., Lohmann, K.C., 1995. $\delta^{18}O$ and $\delta^{13}C$ values of modern brachiopod shells. Geochim. Cosmochim. Acta 59, 3749–3764.

Carpenter, S.J., Lohmann, K.C., 1997. Carbon isotope ratios of Phanerozoic Marine Cements: re-evaluating the global carbon and sulfur systems. Geochim. Cosmochim. Acta 61, 4831–4846.

Carpenter, S.J., Lohman, K.C., Holden, P., Walter, L.M., Houston, T.J., Halliday, A.N., 1991. $\delta^{18}O$ values, $^{87}Sr/^{86}Sr$ and Sr/Mg ratios of Late Devonian abiotic marine calcite: implications for the composition of ancient seawater. Geochim. Cosmochim. Acta 55, 1991–2010.

Carpenter, S.J., Lee, D., McConnaughey, T., Anderson, H., West, H., 1997. Calcareous algae — a new CO_2 barometer: preliminary data from Biosphere 2. Geol. Soc. Am. Annu. Meet. Prog. Abstr. A 396.

Clark, I.D., Fontes, J.-C., Fritz, P., 1992. Stable isotope disequilibria in travertine from high pH waters: laboratory investigations and field observations from Oman. Geochim. Cosmochim. Acta 56, 2041–2050.

Colombo, P.M., 1978. An ultrastructural study of thallus organization in *Udotea petiolata*. Phycologia 17 (3), 227–235.

Cummings, C.E., McCarty, H.B., 1982. Stable carbon isotope ratios in *Astrangia danae*: evidence for algal modification of carbon pools used in calcification. Geochim. Cosmochim. Acta 46, 1125–1129.

Curry, W.B., Duplessy, J.C., Labeyrie, L.D., Shackleton, N.J., 1988. Changes in the distribution of $\delta^{13}C$ of deep water ΣCO_2 between the last glaciation and the Holocene. Paleoceanography 3 (3), 317–341.

Davies, T.A., Worsely, T.R., 1981. Paleoenvironmental implications of oceanic carbonate sedimentation rates. Soc. Econ. Paleontol. Mineral. Spec. Publ. 32, 169–179.

Dawes, C.J., 1981. Marine Botany. Wiley, New York.

DeNiro, M.J., Epstein, S., 1978. Influence of diet on the distribution of carbon isotopes in animals. Geochim. Cosmochim. Acta 42, 495–506.

DeNiro, M.J., Epstein, S., 1979. Relationship between the oxygen isotope ratios of terrestrial plant cellulose, carbon dioxide, and water. Science 204, 51–53.

de Villiers, S., Shen, G.T., Nelson, B.K., 1994. The Sr/Ca temperature relationship in coralline aragonite: influence of variability in $(Sr/Ca)_{seawater}$ and skeletal growth parameters. Geochim. Cosmochim. Acta 58, 197–208.

Digby, P.S.B., 1977. Photosynthesis and respiration in the coralline algae, *Clathromorphum Circumscriptum* and *Corallina officinalis* and the metabolic basis of calcification. J. Mar. Biol. Assoc. UK 57, 1111–1124.

Drever, J.I., Li, Y.H., Maynard, J.B., 1988. Geochemical cycles: the continental crust and the oceans. In: Gregeor, C.B., Garrels, R.M., Mackenzie, F.T., Maynard, J.B. (Eds.), Chemical Cycles in the Evolution of the Earth. Wiley, New York, pp. 17–53.

Epstein, S., Zeiri, L., 1988. Oxygen and carbon isotope compositions of gases respired by humans. Proc. Natl. Acad. Sci. U. S. A. 85, 1727–1731.

Epstein, S., Thompson, P., Yapp, C.J., 1977. Oxygen and hydrogen isotopic ratios in plant cellulose. Science 198, 1209–1215.

Erez, J., 1978. Vital effect on stable isotope composition seen in foraminifera and coral skeletons. Nature 273, 199–202.

Flajs, G., 1977a. Die ultrastrukturen des kalkalgenskeletts. Paleontologr. Abt. B 160, 69–128.

Flajs, G., 1977b. Skeletal structures of some calcifying algae. In: Flugel, E. (Ed.), Fossil Algae. Springer-Verlag, Berlin, pp. 225–231.

Friedman, I., O'Neil, J.R., 1977. Compilation of stable isotope fractionation factors of geochemical interest. In: Fleisher, N. (Ed.), Data of Geochemistry. USGS Prof. Paper 440KK.

Genot, P., 1991. Cenozoic and recent dasycladales. In: Riding, R. (Ed.), Calcareous Algae and Stromatolites. Springer-Verlag, Berlin, pp. 131–145.

Ginsburg, R.N., James, N.P., 1976. Submarine botryoidal aragonite in Holocene reef limestones, Belize. Geology 4, 431–436.

Ginsburgh, R.N., Marsalek, D.S., Schneidermann, N., 1971. Ultrastructure of carbonate cements in a Holocene algal reef of Bermuda. J. Sediment. Petrol. 41, 472–482.

Gonzalez, L.A., Lohmann, K.C., 1985. Carbon and oxygen isotopic composition of Holocene reefal carbonates. Geology 13, 811–814.

Graham, D., Smilie, R.M., 1976. Carbonate dehydratase in marine organisms of the Great Barrier Reef. Aust. J. Plant Physiol. 3, 113–119.

Gross, M.G., 1964. Variations in the $^{18}O/^{16}O$ and $^{13}C/^{12}C$ ratios of diagenetically altered limestones in the Bermuda Islands. J. Geol. 72, 170–194.

Gross, M.G., Tracey, J.I., 1966. Oxygen and carbon isotopic composition of limestones and dolomites, Bikini and Eniwetok Atolls. Science 151, 1082–1084.

Grossman, E.L., 1987. Stable isotopes in modern benthic Foraminifera: a study of vital effect. J. Foraminiferal Res. 17 (1), 48–61.

Hillis, L., 1991. Recent calcified Halimedaceae. In: Riding, R. (Ed.), Calcareous Algae and Stromatolites. Springer-Verlag, Berlin, pp. 167–188.

Hillis-Colinvaux, L., 1980. Ecology and taxonomy of *Halimeda*: primary producer of coral reefs. In: Blaxter, J.H.S., Russel, F.S., Yonge, M. (Eds.), Advances in Marine Biology vol. 17. Academic Press, London, pp. 1–327.

Holmes, C.W., 1983. $\delta^{18}O$ variations in the *Halimeda* of Virgin

Islands sands: evidence of cool water in the northeast Caribbean, late Holocene. J. Sediment. Petrol. 53, 429–438.
James, N.P., Marszalek, D., Choquette, P., 1976. Facies and fabric specificity of early subsea cements in shallow Belize (British Honduras) reefs. J. Sediment. Petrol. 46, 523–544.
Jensen, P.R., Gibson, R.A., Littler, M.M., Littler, D.S., 1985. Photosynthesis and calcification in four deep water *Halimeda* species (Chlorophyceae Caulerpales). Deep-Sea Res. 32 (4), 451–464.
Johansen, H.W., 1981. Coralline Algae, A First Synthesis. CRC Press, Boca Raton, FL.
Keith, M.L., Weber, J.N., 1965. Systematic relationships between carbon and oxygen isotopes in carbonates deposited by modern corals and algae. Science 150, 498–501.
Kinsey, D.W., Hopley, D., 1991. The significance of coral reefs as global carbon sinks-response to Greenhouse. Palaeogeogr., Palaeoclimatol., Palaeoecol. (Global and Planetary Change Section) 89, 363–377.
Ku, T.L., Luo, S., 1992. Carbon isotopic variations on glacial-to-interglacial time scales in the ocean: modeling and implications. Paleoceanography 7 (5), 543–562.
Land, L.S., Goreau, T.F., 1970. Submarine lithification of Jamaican reefs. J. Sediment. Petrol. 40, 457–462.
LaVelle, J.M., 1979. Translocation in *Calliathron tuberculosum* and its role in the light enhancement of calcification. Mar. Biol. 55, 37–44.
Lee, D., Carpenter, S.J., McConnaughey, T., 1997. $\delta^{13}C$ values of carbonates and associated organic matter from calcareous algae grown under variable atmospheric [CO_2] in the Biosphere 2 ocean. Geol. Soc. Am. Annu. Meet. Prog. Abstr. A 396.
Lorens, R.B., 1981. Sr, Cd, Mn and Co distribution coefficients in calcite as a function of calcite precipitation rate. Geochim. Cosmochim. Acta 45, 553–561.
Lowenstam, H.A., Epstein, S., 1957. On the origin of sedimentary aragonite needles of the great Bahama Bank. J. Geol. 65, 364–375.
Macintyre, I.G., Reid, R.P., 1995. Crystal alteration in a living calcareous alga (*Halimeda*): implications for studies in skeletal diagenesis. J. Sediment. Res., Sect. A 65 (1), 143–153.
Marszalek, D.S., 1971. Skeletal ultrastructure of sediment producing green algae. In: Johari, O., Corvin, T. (Eds.), Scanning Electron Microscopy I. Illinois Institute of Technology Research Institute, Chicago, pp. 273–280.
Marszalek, D.S., 1975. Calcisphere ultrastructure and skeletal aragonite from the alga, *Acetabularia antillana*. J. Sediment. Petrol. 45 (1), 266–271.
McConnaughey, T., 1989a. ^{13}C and ^{18}O isotopic disequilibrium in biological carbonates: I. Patterns. Geochim. Cosmochim. Acta 53, 151–162.
McConnaughey, T., 1989b. ^{13}C and ^{18}O isotopic disequilibrium in biological carbonates: II. In vitro simulation of kinetic isotope effects. Geochim. Cosmochim. Acta 53, 163–171.
McConnaughey, T., 1989c. Biomineralization mechanisms. In: Crick, F.C. (Ed.), The Origin, Evolution, and Modern Aspects of Biomineralization in Animals and Plants. Plenum Press, New York, pp. 57–73.
McConnaughey, T., Burdett, J., Whelan, J.F., Paull, C.K., 1997. Carbon isotopes in biological carbonates: respiration and photosynthesis. Geochim. Cosmochim. Acta 61, 611–622.
Milliman, J.D., 1974. Marine Carbonates. Springer-Verlag, New York.
Milliman, J.D., 1993. Production and accumulation of calcium carbonate in the ocean: budget of a nonsteady state. Global Biogeochem. Cycles 7 (4), 927–957.
Moberly Jr., R., 1968. Composition of magnesian calcites of algae and pelecypods by electron microprobe analysis. Sedimentology 11, 61–82.
Multer, H.G., 1988. Growth rate, ultrastructure and sediment contribution of *Halimeda incrassata* and *Halimeda monile*, Nonsuch and Falmouth Bays, Antigua, WI. Coral Reefs 6, 179–186.
Okazaki, M., Ichikawa, K., Furuya, K., 1982. Studies on the calcium carbonate deposition of algae: IV. Initial calcification site of calcareous red alga, *Galaxaura fastigiata* Decaisne. Bot. Mar. 25, 511–517.
O'Leary, M.H., 1984. Measurement of the isotope fractionation associated with diffusion of carbon dioxide in aqueous solution. J. Phys. Chem. 88, 823–825.
O'Leary, M.H., 1988. Carbon isotopes in photosynthesis. BioScience 38 (5), 328–336.
Opdyke, B.N., Walker, J.C.G., 1992. Return of the coral reef hypothesis: basin to shelf partitioning of $CaCO_3$ and its effect on atmospheric CO_2. Geology 20, 733–736.
Paneth, P., O'Leary, M.H., 1985. Carbon isotope effect on dehydration of bicarbonate ion catalyzed by carbonic anhydrase. Biochemistry 24, 5143–5147.
Patterson, W.P., Walter, L.M., 1994. Depletion of ^{13}C in seawater ΣCO_2 on modern carbonate platforms: significance for the carbon isotope record of carbonates. Geology 22, 885–888.
Pearse, V.B., 1972. Radioisotopic study of calcification in the articulated coralline alga, *Bossiella orbigniana*. J. Phycol. 8, 88–97.
Pentecost, A., 1978. Calcification and photosynthesis in *Corallina officinalis* L. using the $^{14}CO_2$ method. Br. Phycol. J. 13, 383–390.
Porter, J.W., Fitt, W.K., Spero, H.J., Rogers, C.S., White, M.W., 1989. Bleaching in reef corals: physiological and stable isotopic responses. Proc. Natl. Acad. Sci. U. S. A. 86, 9342–9346.
Puiseux-Dao, S., 1970. *Acetabularia* and Cell Biology. Logos Press, London.
Romanek, C.S., Grossman, E.L., Morse, J.W., 1992. Carbon isotopic fractionation in synthetic aragonite and calcite: effects of temperature and precipitation rate. Geochim. Cosmochim. Acta 56, 419–430.
Schlanger, S.O., 1988. Strontium storage and release during deposition and diagenesis of marine carbonates related to sea level variations. In: Lerman, A., Meybeck, M. (Eds.), Physical and Chemical Weathering in Geochemical Cycles. Kluwer Academic Publishers, Dordrecht, pp. 323–339.
Shackleton, N.J., 1977. Tropical rainforest history and the equatorial Pacific carbonate dissolution cycles. In: Anderson, N.R., Malahoff, A. (Eds.), The Fate of Fossil Fuel CO_2 in the Oceans, pp. 401–418.
Spero, H.J., Lerche, I., Williams, D.F., 1991. Opening the carbon

isotope "vital effect" black box: 2. Quantitative model for interpreting foraminiferal carbon isotope data. Paleoceanography 6, 639–655.

Spero, H.J., Bijma, J., Lea, D.W., Bemis, B.E., 1997. Effect of seawater carbonate concentration on foraminiferal carbon and oxygen isotopes. Nature 390, 497–500.

Stark, L.M., Almodovar, L., Krauss, R.W., 1969. Factors affecting the rate of calcification in *Halimeda opuntia* (L) Lamouroux and *Halimeda discoidea* Decaisne. J. Phycol. 5, 305–312.

Sultemeyer, D., Rinast, K.A., 1996. The CO_2 permeability of the plasma membrane of *Chlamydomonas reinhardtii*: mass spectrometric ^{18}O exchange measurements from $^{13}C^{18}O_2$ in suspensions of carbonic anhydrase-loaded plasma membrane vesicles. Planta 200, 358–368.

Swart, P.K., 1983. Carbon and oxygen isotope fractionation in Scleractinian corals: a review. Earth Sci. Rev. 19, 51–80.

Tanaka, N., Monaghan, M.C., Rye, D.M., 1986. Contribution of metabolic carbon to mollusc and barnacle shell carbonate. Nature 320, 520–523.

Tarutani, T., Clayton, R.N., Mayeda, T.K., 1969. The effect of polymorphism and magnesium substitution on oxygen isotope fractionation between calcium carbonate and water. Geochim. Cosmochim. Acta 33, 987–996.

Toomey, D.F., Nitecki, M.H., 1985. Paleoalgology: Contemporary Research and Applications. Springer-Verlag, Berlin.

Urey, H.C., Lowenstam, H.A., Epstein, S., McKinney, C.R., 1951. Measurement of paleotemperatures and temperatures of the upper Cretaceous of England, Denmark, and the southeastern United States. Bull. Geol. Soc. Am. 62, 399–416.

Walker, J.C.G., Opdyke, B.C., 1995. Influence of variable rates of neritic carbonate deposition on atmospheric carbon dioxide and pelagic sediments. Paleoceanography 10, 415–427.

Wang, J., Carpenter, S.J., McConnaughey, T., 1995. Systematic variations in the ^{18}O and ^{13}C values of *Acropora palmata* and *Acropora cervicornis* aragonite: implications for coral physiology and biomineralization. Geol. Soc. Am. Annu. Meet. Prog. Abstr. A 158.

Weber, J.N., Raup, D.M., 1966a. Fractionation of the stable isotopes of carbon and oxygen in marine calcareous organisms — the Echinoidea: Part I. Variation of ^{13}C and ^{18}O content within individuals. Geochim. Cosmochim. Acta 30, 681–703.

Weber, J.N., Raup, D.M., 1966b. Fractionation of the stable isotopes of carbon and oxygen in marine calcareous organisms — the Echinoidea. Part II. Environmental and genetic factors. Geochim. Cosmochim. Acta 30, 705–736.

Wefer, G., Berger, W.H., 1981. Stable isotopic composition of benthic calcareous algae from Bermuda. J. Sediment. Petrol. 51, 459–465.

Wefer, G., Berger, W.H., 1991. Isotope paleontology: growth and composition of extant calcareous species. Mar. Geol. 100, 207–248.

Wilbur, K.M., Colinvaux, L.H., Watabe, N., 1969. Electron microscope study of calcification in the alga *Halimeda* (order: Siphonales). Phycologia 8 (1), 27–35.